

This content has been downloaded from IOPscience. Please scroll down to see the full text.

Download details:

IP Address: 18.117.73.223

This content was downloaded on 05/05/2024 at 21:19

Please note that [terms and conditions apply](#).

You may also like:

# Chapter 8

## Multiparticle systems

*This chapter provides a brief introduction to quantum mechanics of systems of similar particles, with special attention on the case when they are indistinguishable. For such systems, theory predicts (and experiment confirms) very specific effects, even in the case of negligible explicit ('direct') interaction between the particles. These effects notably include the Bose–Einstein condensation of bosons, and the exchange interaction of fermions.*

### 8.1 Distinguishable and indistinguishable particles

The importance of quantum systems of many similar particles is probably self-evident; just the very fact that most atoms include several/many electrons is sufficient to attract our attention. There are also important systems where the number of electrons is much higher than in one atom; for example, a cubic centimeter of a typical metal houses  $\sim 10^{23}$  conduction electrons that cannot be attributed to particular atoms, and have to be considered as common parts of the system as the whole. Though quantum mechanics offers virtually no exact analytical results for systems of substantially interacting particles<sup>1</sup>, it reveals very important new quantum effects even in the simplest case when particles do not interact, and least explicitly (*directly*).

If non-interacting particles are either different from each other by their nature, or physically similar but still *distinguishable* because of other reasons, everything is simple—at least, conceptually. Then, as was already discussed in section 6.7, a

---

<sup>1</sup> As was emphasized in section 7.3, for such systems of similar particles the powerful methods discussed in the last chapter, based on the separation of the whole Universe into the 'system of our interest' and the 'environment', typically do not work well—mostly because the quantum state of the 'particle of interest' may be substantially correlated (in particular, entangled) with those of similar particles of its 'environment'—see below.

system of two particles, 1 and 2, each in a pure quantum state, may be described by a ket-vector being a direct product,

$$|\alpha\rangle = |\beta\rangle_1 \otimes |\beta'\rangle_2, \quad (8.1a)$$

of the single-particle ket-vectors, describing their states  $\beta$  and  $\beta'$  defined in different Hilbert spaces. (Below, I will frequently use, for the direct product, the following convenient shorthand:

$$|\alpha\rangle = |\beta\beta'\rangle, \quad (8.1b)$$

in which the state symbol's position within the vector codes the particle's number.) Hence the *permuted state*

$$\hat{\mathcal{P}}|\beta\beta'\rangle \equiv |\beta'\beta\rangle \equiv |\beta'\rangle_1 \otimes |\beta\rangle_2, \quad (8.2)$$

where  $\hat{\mathcal{P}}$  is the *permutation operator* (defined by this equality), is clearly different from the initial one.

Such operator may be also used for states of systems of *identical particles*. This term may be used to describe:

(i) the ‘really elementary’ particles like electrons, which (at least at this stage of development of physics) are considered as structure-less entities, and hence are all identical;

(ii) any objects (e.g. hadrons or mesons) that may be considered as a system of ‘more elementary’ particles (e.g. quarks and gluons), but still are reliably placed in the same quantum state—most simply, though not necessarily, to the ground state<sup>2</sup>.

It is important to note that identical particles still may be *distinguishable*—say by their clear spatial separation. Such systems of similar but distinguishable particles (or subsystems) are broadly discussed nowadays, for example in the context of quantum computing and encryption—see section 8.5 below. This is why it is insufficient to use the term ‘identical particles’ if we want to say that they are genuinely *indistinguishable*, so below I will use the latter term, despite it being rather unpleasant grammatically.

It turns out that for a quantitative description of systems of indistinguishable particles we need to use, instead of direct products of the type (8.1), linear combinations of products such products, for example of  $|\beta\beta'\rangle$  and  $|\beta'\beta\rangle$ .<sup>3</sup> To see

<sup>2</sup>Note that from this point of view, even complex atoms or molecules, in the same quantum state, may be considered on the same footing as the ‘really elementary’ particles. For example, the already mentioned recent spectacular interference experiments by R Lopes *et al*, which require particle identity, were carried out with couples of <sup>4</sup>He atoms in the same internal state.

<sup>3</sup>A very legitimate question is why, in this situation, we need to introduce the particles’ numbers to start with. A partial answer is that in this approach, it is much simpler to derive (or guess) the system Hamiltonians from the correspondence principle—see, e.g. Eq. (8.27) below. Later in this chapter, we will discuss an alternative approach (the so-called ‘second quantization’), in which particle numbering is avoided. While this approach is more logical, writing adequate Hamiltonians (which, in particular, would avoid spurious self-interaction of the particles) in it is much more challenging—see section 8.3 below.

this, let us discuss properties of the permutation operator defined by Eq. (8.2). Consider an observable  $A$ , and a system of eigenstates of its operator:

$$\hat{A}|a_j\rangle = A_j|a_j\rangle. \quad (8.3)$$

If the particles are indistinguishable, the observable's expectation value should not be affected by their permutation. Hence the operators  $\hat{A}$  and  $\hat{\mathcal{P}}$  have to commute, and share their eigenstates. This is why eigenstates of the operator  $\hat{\mathcal{P}}$  are so important: in particular, they include the eigenstates of the Hamiltonian, i.e. the stationary states of a system of indistinguishable particles.

Let us have a look at the action of the permutation operator squared, on an elementary ket-vector product:

$$\hat{\mathcal{P}}^2|\beta\beta'\rangle = \hat{\mathcal{P}}(\hat{\mathcal{P}}|\beta\beta'\rangle) = \hat{\mathcal{P}}|\beta'\beta\rangle = |\beta\beta'\rangle, \quad (8.4)$$

i.e.  $\hat{\mathcal{P}}^2$  brings the state back to its original form. Since any pure state of a two-particle system may be represented as a linear combination of such products, this result does not depend on the state, and may be represented as the following operator relation:

$$\hat{\mathcal{P}}^2 = \hat{I}. \quad (8.5)$$

Now let us find the possible eigenvalues  $\mathcal{P}_j$  of the permutation operator. Acting by both sides of Eq. (8.5) on any of eigenstates  $|\alpha_j\rangle$  of the permutation operator, we get a very simple equation for its eigenvalues:

$$\mathcal{P}_j^2 = 1, \quad (8.6)$$

with two possible solutions:

$$\mathcal{P}_j = \pm 1. \quad (8.7)$$

Let us find the eigenstates of the permutation operator in the simplest case when each of the component particles can be only in one of two single-particle states—say,  $\beta$  and  $\beta'$ . Evidently, none of the simple products  $|\beta\beta'\rangle$  and  $|\beta'\beta\rangle$ , taken alone, does qualify for the eigenstate—unless the states  $\beta$  and  $\beta'$  are identical. For this reason let us try their linear combination

$$|\alpha_j\rangle = a|\beta\beta'\rangle + b|\beta'\beta\rangle, \quad (8.8)$$

so that

$$\hat{\mathcal{P}}|\alpha_j\rangle = \mathcal{P}_j|\alpha_j\rangle = a|\beta'\beta\rangle + b|\beta\beta'\rangle. \quad (8.9)$$

For the case  $\mathcal{P}_j = +1$  we have to require the states (8.8) and (8.9) to be the same, so that  $a = b$ , giving the so-called *symmetric eigenstate*<sup>4</sup>

---

<sup>4</sup>As in many situations we have met earlier, the kets given by Eqs. (8.10) and (8.11) may be multiplied by  $\exp\{i\varphi\}$  with an arbitrary real phase  $\varphi$ . However, until we discuss coherent superpositions of various states  $\alpha$ , there is no good motivation for taking the phase different from 0; that would only clutter the notation.

$$|\alpha_+\rangle = \frac{1}{\sqrt{2}}(|\beta\beta'\rangle + |\beta'\beta\rangle), \quad (8.10)$$

where the front coefficient guarantees the orthonormality of the two-particle state, provided that the single-particle states are orthonormal. Similarly, for  $\mathcal{P}_j = -1$  we get  $a = -b$ , i.e. an *antisymmetric eigenstate*

$$|\alpha_-\rangle = \frac{1}{\sqrt{2}}(|\beta\beta'\rangle - |\beta'\beta\rangle). \quad (8.11)$$

These are the simplest (two-particle, two-state) examples of *entangled states*, defined as multiparticle system's states whose vectors cannot be factored into a direct product (8.1) of single-particle vectors.

So far, our math does not preclude either sign of  $\mathcal{P}_j$ , in particular the possibility that the sign depends on the state (i.e. on the index  $j$ ). Here, however, comes in a crucial *experimental* fact: all indistinguishable particles fall into two groups<sup>5</sup>:

- (i) *bosons*, particles with integer spin  $s$ , for whose states  $\mathcal{P}_j = +1$ , and
- (ii) *fermions*, particles with half-integer spin, with  $\mathcal{P}_j = -1$ .

In the non-relativistic theory we are discussing now, this key fact should be considered as an experimental one. (The relativistic quantum theory, whose elements will be discussed in chapter 9, offers a proof that the half-integer-spin particles cannot be bosons and the integer-spin ones cannot be fermions.) However, our discussion of spin in section 5.7 enables the following plausible *interpretation* of the fermion–boson difference. In the free space, the permutation of particles 1 and 2 may be viewed as a result of this pair's rotation by angle  $\pm\pi$  about a certain axis. As we have seen in section 5.7, at the rotation by such an angle, the state vector  $|\beta\rangle$  of a particle with a quantum number  $m_s$  (which ranges from  $-s$  to  $+s$ , and hence may take only integer values for integer  $s$ , and only half-integer values for half-integer  $s$ ) changes by the factor  $\exp\{\pm i\pi m_s\}$ , so that the state product  $|\beta\beta'\rangle$  has to change by  $\exp\{\pm i2\pi m_s\}$ , i.e. by the factor  $+1$  for any integer  $s$ , and by the factor  $(-1)$  for any half-integer  $s$ .

The most impressive corollaries of Eqs. (8.10) and (8.11) are for the case when the partial states of the two particles are the same:  $\beta = \beta'$ . The corresponding Bose state  $\alpha_+$  is possible; in particular, at sufficiently low temperatures, a set of non-interacting Bose particles condenses on the ground state of each of them—the so-called *Bose–Einstein condensate* ('BEC').<sup>6</sup> Perhaps the most fascinating feature of a Bose–Einstein condensate is that the dynamics of its observables is governed by laws of

<sup>5</sup> Sometimes this fact is described as having two different 'statistics': the *Bose–Einstein statistics* of bosons, and *Fermi–Dirac statistics* of fermions, because their statistical distributions in thermal equilibrium are indeed different—see, e.g. *Part SM* section 2.8. However, this difference is actually deeper: we are dealing with *two different quantum mechanics*.

<sup>6</sup> For a quantitative discussion of the Bose–Einstein condensation see, e.g. *Part SM* section 3.4. Examples of such condensates include *superfluids* like helium, Cooper-pair condensates in superconductors, and BECs of weakly interacting atoms.

quantum mechanics, while (for nearly all purposes) they may be treated as  $c$ -numbers—see, e.g. Eqs. (1.73) and (1.74).<sup>7</sup>

On the other hand, if we take  $\beta = \beta'$  in Eq. (8.11), we see that state  $\alpha_-$  becomes the null-state, i.e. *cannot exist* at all. This is the mathematical expression of the *Pauli exclusion principle*<sup>8</sup>: two indistinguishable fermions cannot be in the same quantum state. (As will be discussed below, this is true for systems with more than two fermions as well.) Probably, the key importance of this principle is self-evident: if it was not valid for electrons (that are fermions), all electrons of each atom would condense on its ground ( $1s$ -like) level, and all the usual chemistry (and biochemistry, and biology, including dear us!) would not exist. The Pauli principle makes fermions implicitly interacting even if they do not interact *directly*, i.e. in the usual sense of this word.

## 8.2 Singlets, triplets, and the exchange interaction

Now let us discuss possible approaches to quantitative analyses of identical particles, starting from a simple case of two spin- $1/2$  particles (say, electrons), whose interaction with each other and the external world does not involve spin. The description of such a system may be based on factorable states with ket-vectors

$$|\alpha_-\rangle = |o_{12}\rangle \otimes |s_{12}\rangle, \quad (8.12)$$

with the orbital function  $|o_{12}\rangle$  and the spin function  $|s_{12}\rangle$  (that depends on the state of both spins of the pair) belonging to different Hilbert spaces. It is frequently convenient to use the coordinate representation of such a state, sometimes called the *spinor*:

$$\langle \mathbf{r}_1, \mathbf{r}_2 | \alpha_- \rangle = \langle \mathbf{r}_1, \mathbf{r}_2 | o_{12} \rangle \otimes |s_{12}\rangle \equiv \psi(\mathbf{r}_1, \mathbf{r}_2) |s_{12}\rangle. \quad (8.13)$$

Since the spin- $1/2$  particles are fermions, the particle permutation has to change the sign:

$$\hat{\mathcal{P}}\psi(\mathbf{r}_1, \mathbf{r}_2) |s_{12}\rangle \equiv \psi(\mathbf{r}_2, \mathbf{r}_1) |s_{21}\rangle = -\psi(\mathbf{r}_1, \mathbf{r}_2) |s_{12}\rangle, \quad (8.14)$$

of either the orbital factor of the spinor, or its spin factor.

In particular, in the case of a symmetric orbital factor,

$$\psi(\mathbf{r}_2, \mathbf{r}_1) = \psi(\mathbf{r}_1, \mathbf{r}_2), \quad (8.15)$$

the spin factor has to obey the relation

$$|s_{21}\rangle = -|s_{12}\rangle. \quad (8.16)$$

<sup>7</sup> For example, for the Bose–Einstein condensate of  $N \gg 1$  particles, the Heisenberg uncertainty relation may be reduced to  $\delta N \delta \varphi > 1$ , where  $\varphi$  is the condensate wavefunction’s phase, so that it may have  $\delta N / \langle N \rangle \ll 1$  and  $\delta \varphi \ll 1$  simultaneously.

<sup>8</sup> It was formulated by W Pauli in 1925, on the basis of less general rules suggested by G Lewis (1916), I Langmuir (1919), N Bohr (1922), and E Stoner (1924) for the explanation of experimental spectroscopic data.

Let us use the ordinary  $z$ -basis (where  $z$ , in the absence of external magnetic field, is an arbitrary spatial axis) for both spins. In this basis, the ket-vector of any two-spin state may be represented as a linear combination of the four following basis vectors:

$$|\uparrow\uparrow\rangle, \quad |\downarrow\downarrow\rangle, \quad |\uparrow\downarrow\rangle, \quad \text{and} \quad |\downarrow\uparrow\rangle. \quad (8.17)$$

The first two kets evidently do not satisfy Eq. (8.16), and cannot participate in the state. Applying to the remaining kets the same argumentation as has resulted in Eq. (8.11), we get

$$|s_{12}\rangle = |s_{-}\rangle \equiv \frac{1}{\sqrt{2}}(|\uparrow\downarrow\rangle - |\downarrow\uparrow\rangle). \quad (8.18)$$

Such an orbital-symmetric and spin-asymmetric state is called the *singlet*.

The origin of this term becomes clear from the analysis of the opposite (orbital-asymmetric and spin-symmetric) case:

$$\psi(\mathbf{r}_2, \mathbf{r}_1) = -\psi(\mathbf{r}_1, \mathbf{r}_2), \quad |s_{12}\rangle = |s_{21}\rangle. \quad (8.19)$$

For the composition of such a symmetric spin state, the first two kets of Eq. (8.17) are completely acceptable (with arbitrary weights), and so is an entangled spin state that is a symmetric combination of the two last kets, similar to Eq. (8.10):

$$|s_{+}\rangle \equiv \frac{1}{\sqrt{2}}(|\uparrow\downarrow\rangle + |\downarrow\uparrow\rangle), \quad (8.20)$$

so that the general spin state is a *triplet*:

$$|s_{12}\rangle = c_{+} |\uparrow\uparrow\rangle + c_{-} |\downarrow\downarrow\rangle + c_0 \frac{1}{\sqrt{2}}(|\uparrow\downarrow\rangle + |\downarrow\uparrow\rangle). \quad (8.21)$$

Note that such a state, with values of the coefficients  $c$  (satisfying the normalization condition), corresponds to the same orbital wavefunction and hence the same energy. However, each of these three states has a specific value of the  $z$ -component of the net spin—evidently equal to, respectively,  $+\hbar$ ,  $-\hbar$ , and 0. Because of this, even a small external magnetic field lifts their degeneracy, splitting the energy level in three; hence the term ‘triplet’.

In the particular case when the particles do not interact at all, for example

$$\hat{H} = \hat{h}_1 + \hat{h}_2, \quad \hat{h}_k = \frac{\hat{p}_k^2}{2m} + \hat{u}(\mathbf{r}_k), \quad \text{with } k = 1, 2, \quad (8.22)$$

the two-particle Schrödinger equation for the symmetrical orbital wavefunction (8.15) is obviously satisfied by the direct products,

$$\psi(\mathbf{r}_1, \mathbf{r}_2) = \psi_n(\mathbf{r}_1)\psi_{n'}(\mathbf{r}_2), \quad (8.23)$$

of single-particle eigenfunctions, with arbitrary sets  $n, n'$  of quantum numbers. For the particular but very important case  $n = n'$ , this means that the eigenenergy of the (only acceptable) singlet state,

$$\frac{1}{\sqrt{2}}(|\uparrow\downarrow\rangle - |\downarrow\uparrow\rangle)\psi_n(\mathbf{r}_1)\psi_n(\mathbf{r}_2), \quad (8.24)$$

is just  $2\varepsilon_n$ , where  $\varepsilon_n$  is the single-particle energy level<sup>9</sup>. In particular, for the ground state of the system, such singlet spin state gives the lowest energy  $E_g = 2\varepsilon_g$ , while any triplet spin state (8.19) would require one of the particles to be in a different orbital state, i.e. in a state of higher energy, so that the total energy of the system would be also higher.

Now moving to the systems in which two indistinguishable spin- $1/2$  particles do interact, let us consider, as their simplest but important<sup>10</sup> example, the lower energy states of a neutral atom<sup>11</sup> of helium—more exactly,  ${}^4\text{He}$ . Such an atom consists of a nucleus with two protons and two neutrons, with the total electric charge  $q = +2e$ , and two electrons ‘rotating’ about the nucleus. Neglecting the small relativistic effects that were discussed in section 6.3, the Hamiltonian describing the electron motion may be expressed as

$$\hat{H} = \hat{h}_1 + \hat{h}_2 + \hat{U}_{\text{int}}, \quad \hat{h}_k = \frac{\hat{p}_k^2}{2m} - \frac{2e^2}{4\pi\varepsilon_0 r_k}, \quad \hat{U}_{\text{int}} = \frac{e^2}{4\pi\varepsilon_0 |\mathbf{r}_1 - \mathbf{r}_2|}. \quad (8.25)$$

As most problems of multiparticle quantum mechanics, the eigenvalue/eigenstate problem for this Hamiltonian does not have an exact analytical solution, so let us carry out its approximate analysis considering the electron–electron interaction  $U_{\text{int}}$  as a perturbation. As was discussed in chapter 6, we have to start with the ‘0th-order’ approximation in which the perturbation is ignored, so that the Hamiltonian is reduced to the sum (8.22). In this approximation, the ground state of the atom is the singlet (8.24), with the orbital factor

$$\psi_g(\mathbf{r}_1, \mathbf{r}_2) = \psi_{100}(\mathbf{r}_1)\psi_{100}(\mathbf{r}_2), \quad (8.26)$$

and the energy  $2\varepsilon_g$ . Here each factor  $\psi_{100}(\mathbf{r})$  is the single-particle wavefunction of the ground ( $1s$ ) state of the hydrogen-like atom with  $Z = 2$ , with quantum numbers  $n = 1$ ,  $l = 0$ ,  $m = 0$ . According to Eqs. (3.174) and (3.208),

$$\psi_{100}(\mathbf{r}) = Y_0^0(\theta, \varphi) \mathcal{R}_{1,0}(r) = \frac{1}{\sqrt{4\pi}} \frac{2}{r_0^{3/2}} e^{-r/r_0}, \quad \text{with } r_0 = \frac{r_B}{Z} = \frac{r_B}{2}, \quad (8.27)$$

so that according to Eqs. (3.191) and (3.201), in this approximation the total ground state energy is

$$E_g^{(0)} = 2\varepsilon_g^{(0)} = 2\left(-\frac{\varepsilon_0}{2n^2}\right)_{n=1, Z=2} = 2\left(-\frac{Z^2 E_H}{2}\right)_{Z=2} = -4E_H \approx -109 \text{ eV}. \quad (8.28)$$

<sup>9</sup>In this chapter, I try to use lower-case letters for all single-particle observables (in particular,  $\varepsilon$  for their energies), in order to distinguish them as clearly as possible from system’s observables (including the total energy  $E$  of the system), typeset in capital letters.

<sup>10</sup>Indeed, helium makes up more than 20% of all ‘ordinary’ matter of our Universe.

<sup>11</sup>Evidently, the positive ion  $\text{He}^{+1}$  of this atom, with just one electron, is fully described by the hydrogen-like atom theory with  $Z = 2$ , whose ground-state energy, according to Eq. (3.191), is  $-Z^2 E_H/2 = -2E_H \approx -55.4 \text{ eV}$ .



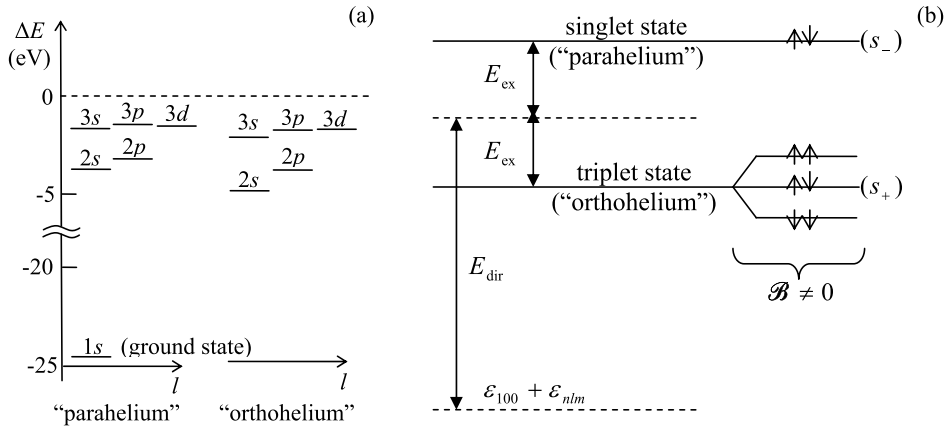


**Figure 8.1.** The lower energy levels of a helium atom: (a) experimental data and (b) a schematic structure of an excited state in the first order of the perturbation theory. On panel (a), all energies are referred to that  $(-2E_H \approx -55.4 \text{ eV})$  of the ground state of the positive ion  $\text{He}^{+1}$ , so that their magnitudes are the (readily measurable) energies of atom's ionization starting from the corresponding bound state. Note that the 'spin direction' nomenclature on panel (b) is rather crude: it does not reflect the difference between the entangled states  $s_+$  and  $s_-$ .

This is still somewhat far (though not terribly far!) from the experimental value  $E_g \approx -78.8 \text{ eV}$ —see the bottom level in figure 8.1a.

Making a small (but useful) detour from our main topic, let us note that we can get a much better agreement with experiment by calculating the electron interaction energy in the 1st order of the perturbation theory. Indeed, in application to our system, Eq. (6.14) reads

$$E_g^{(1)} = \langle g | \tilde{U}_{\text{int}} | g \rangle = \int d^3r_1 \int d^3r_2 \psi_g^*(\mathbf{r}_1, \mathbf{r}_2) U_{\text{int}}(\mathbf{r}_1, \mathbf{r}_2) \psi_g(\mathbf{r}_1, \mathbf{r}_2). \quad (8.29)$$

Plugging in Eqs. (8.25)–(8.27), we get

$$E_g^{(1)} = \left( \frac{1}{4\pi} \frac{4}{r_0^3} \right)^2 \int d^3r_1 \int d^3r_2 \frac{e^2}{4\pi\epsilon_0 |\mathbf{r}_1 - \mathbf{r}_2|} \exp \left\{ -\frac{2(r_1 + r_2)}{r_0} \right\}. \quad (8.30)$$

As may be readily evaluated analytically (this exercise is left for the reader), this expression equals  $(5/4)E_H$ , so that the corrected ground state energy,

$$E_g \approx E_g^{(0)} + E_g^{(1)} = (-4 + 5/4)E_H = -74.8 \text{ eV}, \quad (8.31)$$

is much closer to experiment.

There is still room for ready improvement, using the variational method discussed in section 2.9. For our particular case of a  $^4\text{He}$  atom, we may try to use, as the trial state, the wavefunction given by Eqs. (8.26) and (8.27), but with the atomic number

$Z$  considered as an adjustable parameter  $Z_{\text{ef}} < Z = 2$  rather than a fixed number. The physics behind this approach is that the electric charge density  $\rho(\mathbf{r}) = -e|\psi(\mathbf{r})|^2$  of each electron forms a negatively charged ‘cloud’ that reduces the effective charge of the nucleus, as seen by another electron, to  $Z_{\text{ef}}e^2$ , with some  $Z_{\text{ef}} < 2$ . As a result, the single-particle wavefunction spreads further in space (with the scale  $r_0 = r_{\text{B}}/Z_{\text{ef}} > r_{\text{B}}/Z$ ), while keeping its functional form (8.27) nearly intact. Since the kinetic energy  $T$  in system’s Hamiltonian (8.25) is proportional to  $r_0^{-2} \propto Z_{\text{ef}}^2$ , while the potential energy is proportional to  $r_0^{-1} \propto Z_{\text{ef}}^1$ , we can write

$$E_{\text{g}}(Z_{\text{ef}}) = \left(\frac{Z_{\text{ef}}}{2}\right)^2 \langle T_{\text{g}} \rangle_{Z=2} + \frac{Z_{\text{ef}}}{2} \langle U_{\text{g}} \rangle_{Z=2}. \quad (8.32)$$

Now we can use the fact that according to Eq. (3.212), for any stationary state of a hydrogen-like atom (just as for the classical circular motion in the Coulomb potential),  $\langle U \rangle = 2E$ , and hence  $\langle T \rangle = E - \langle U \rangle = -E$ . Using Eq. (8.30), and adding the correction  $U_{\text{g}}^{(1)} = -(5/4)E_{\text{H}}$ , calculated above, to the potential energy, we get

$$E_{\text{g}}(Z_{\text{ef}}) = \left[ 4\left(\frac{Z_{\text{ef}}}{2}\right)^2 + \left(-8 + \frac{5}{4}\right)\frac{Z_{\text{ef}}}{2} \right] E_{\text{H}}. \quad (8.33)$$

This expression allows an elementary calculation of the optimal value of  $Z_{\text{ef}}$ , and the corresponding minimum of the function  $E_{\text{g}}(Z_{\text{ef}})$ :

$$(Z_{\text{ef}})_{\text{opt}} = 2\left(1 - \frac{5}{32}\right) = 1.6875, \quad (E_{\text{g}})_{\text{min}} \approx -2.85E_{\text{H}} \approx -77.5 \text{ eV}. \quad (8.34)$$

Given the trial state’s crudeness, this number is in a surprisingly good agreement with experimental value cited above, with a difference of the order of 1%.

Now let us return to the basic topic of this section—the effects of particle (in this case, electron) indistinguishability. As we have just seen, the ground level energy of the helium atom is not affected directly by this fact, but the situation is different for its excited states—even the lowest ones. The reasonably good convergence of the perturbation theory, which we have seen for the ground state, tells us that we can base our analysis of wavefunctions ( $\psi_{\text{e}}$ ) of the lowest excited state orbitals, on products like  $\psi_{100}(\mathbf{r}_k)\psi_{nlm}(\mathbf{r}_{k'})$ , with  $n > 1$ . However, in order to satisfy the fermion permutation rule,  $\mathcal{P}_j = -1$ , we have to take the orbital factor of the state in the either symmetric or asymmetric form:

$$\psi_{\text{e}}(\mathbf{r}_1, \mathbf{r}_2) = \frac{1}{\sqrt{2}}[\psi_{100}(\mathbf{r}_1)\psi_{nlm}(\mathbf{r}_2) \pm \psi_{nlm}(\mathbf{r}_1)\psi_{100}(\mathbf{r}_2)], \quad (8.35)$$

with the proper total permutation asymmetry provided by the corresponding spin factor (8.18) or Eq. (8.21), so that the upper/lower sign in Eq. (8.35) corresponds to the singlet/triplet spin state. Let us calculate the expectation values of the total

energy of the system in the first order of the perturbation theory. Plugging Eq. (8.35) into the 0th-order expression

$$\langle E_e \rangle^{(0)} = \int d^3r_1 \int d^3r_2 \psi_e^*(\mathbf{r}_1, \mathbf{r}_2) (\hat{h}_1 + \hat{h}_2) \psi_e(\mathbf{r}_1, \mathbf{r}_2), \quad (8.36)$$

we get two groups of similar terms that differ only by the particle index. We can merge the terms of each pair by changing the notation as  $(\mathbf{r}_1 \rightarrow \mathbf{r}, \mathbf{r}_2 \rightarrow \mathbf{r}')$  in one of them, and  $(\mathbf{r}_1 \rightarrow \mathbf{r}', \mathbf{r}_2 \rightarrow \mathbf{r})$  in the other term. Using Eq. (8.25), and the mutual orthogonality of wavefunctions  $\psi_{100}(\mathbf{r})$  and  $\psi_{nlm}(\mathbf{r})$ , we get the following result:

$$\begin{aligned} \langle E_e \rangle^{(0)} &= \int \psi_{100}^*(\mathbf{r}) \left( -\frac{\hbar^2 \nabla_{\mathbf{r}}^2}{2m} - \frac{2e^2}{4\pi\epsilon_0 r} \right) \psi_{100}(\mathbf{r}) d^3r \\ &+ \int \psi_{nlm}^*(\mathbf{r}') \left( -\frac{\hbar^2 \nabla_{\mathbf{r}'}^2}{2m} - \frac{2e^2}{4\pi\epsilon_0 r'} \right) \psi_{nlm}(\mathbf{r}') d^3r' \equiv \epsilon_{100} + \epsilon_{nlm}. \end{aligned} \quad (8.37)$$

It may be interpreted as the sum of eigenenergies of two separate single particles, one in the ground state 100, and another in the excited state  $nlm$ —despite the fact that actually the electron states are entangled. Thus, in the 0th order of the perturbation theory, the electron entanglement does not affect their energy.

However, the potential energy of the system also includes the interaction term  $U_{\text{int}}$ , which does not allow such separation. Indeed, in the 1st approximation of the perturbation theory, the total energy  $E_e$  of the system may be expressed as  $\epsilon_{100} + \epsilon_{nlm} + E_{\text{int}}^{(1)}$ , with

$$E_{\text{int}}^{(1)} = \langle U_{\text{int}} \rangle = \int d^3r_1 \int d^3r_2 \psi_e^*(\mathbf{r}_1, \mathbf{r}_2) U_{\text{int}}(\mathbf{r}_1, \mathbf{r}_2) \psi_e(\mathbf{r}_1, \mathbf{r}_2), \quad (8.38)$$

Plugging Eq. (8.35) into this result, using the symmetry of the function  $U_{\text{int}}$  with respect to the particle number permutation, and the same particle coordinate re-numbering as above, we get

$$E_{\text{int}}^{(1)} = E_{\text{dir}} \pm E_{\text{ex}}, \quad (8.39)$$

with the following, deceptively similar expressions for the two terms:

$$E_{\text{dir}} \equiv \int d^3r \int d^3r' \psi_{100}^*(\mathbf{r}) \psi_{nlm}^*(\mathbf{r}') U_{\text{int}}(\mathbf{r}, \mathbf{r}') \psi_{100}(\mathbf{r}) \psi_{nlm}(\mathbf{r}'), \quad (8.40)$$

$$E_{\text{ex}} \equiv \int d^3r \int d^3r' \psi_{100}^*(\mathbf{r}) \psi_{nlm}^*(\mathbf{r}') U_{\text{int}}(\mathbf{r}, \mathbf{r}') \psi_{nlm}(\mathbf{r}) \psi_{100}(\mathbf{r}'). \quad (8.41)$$

Since the single-particle orbitals can be always made real, both components are positive (or at least non-negative). However, their physics is completely different. The integral (8.40), called the *direct interaction energy*, allows a simple semi-classical

interpretation as the Coulomb energy of interacting electrons, each distributed in space with the electric charge density  $\rho(\mathbf{r}) = -e\psi^*(\mathbf{r})\psi(\mathbf{r})$ :<sup>12</sup>

$$\begin{aligned} E_{\text{dir}} &= \int d^3r \int d^3r' \frac{\rho_{100}(\mathbf{r})\rho_{nlm}(\mathbf{r}')}{4\pi\epsilon_0|\mathbf{r} - \mathbf{r}'|} \equiv \int \rho_{100}(\mathbf{r})\phi_{nlm}(\mathbf{r})d^3r \\ &\equiv \int \rho_{nlm}(\mathbf{r})\phi_{100}(\mathbf{r})d^3r, \end{aligned} \quad (8.42)$$

where  $\phi(\mathbf{r})$  are the electrostatic potentials created by the electrons' 'electric charge clouds':<sup>13</sup>

$$\phi_{100}(\mathbf{r}) = \frac{1}{4\pi\epsilon_0} \int d^3r' \frac{\rho_{100}(\mathbf{r}')}{|\mathbf{r} - \mathbf{r}'|}, \quad \phi_{nlm}(\mathbf{r}) = \frac{1}{4\pi\epsilon_0} \int d^3r' \frac{\rho_{nlm}(\mathbf{r}')}{|\mathbf{r} - \mathbf{r}'|}. \quad (8.43)$$

However, the integral (8.41), called the *exchange interaction energy*, evades a classical interpretation, and (as is clear from its derivation) is the direct corollary of electrons' indistinguishability. The magnitude of  $E_{\text{ex}}$  is also very much different from  $E_{\text{dir}}$ , because the function under the integral (8.41) disappears in the regions where single-particle wavefunctions do not overlap. This is in a full agreement with the discussion in section 8.1: if two particles are identical but well separated, i.e. their wavefunctions do not overlap, the exchange interaction disappears, i.e. measurable effects of particle indistinguishability vanish.

Figure 8.1b shows the structure of an excited energy level, with certain quantum numbers  $n > 1$ ,  $l$ , and  $m$ , given by Eqs. (8.39)–(8.41). The upper, so-called *parahelium*<sup>14</sup> level, with the energy

$$E_{\text{para}} = (\epsilon_{100} + \epsilon_{nlm}) + E_{\text{dir}} + E_{\text{ex}} > \epsilon_{100} + \epsilon_{nlm}, \quad (8.44)$$

corresponds to the symmetric orbital state and hence to the singlet spin state (8.18), while the lower, *orthohelium* level, with

$$E_{\text{orth}} = (\epsilon_{100} + \epsilon_{nlm}) + E_{\text{dir}} - E_{\text{ex}} < E_{\text{para}}, \quad (8.45)$$

corresponds to the degenerate triplet spin state (8.21). This degeneracy may be lifted by an external magnetic field, whose effect of the electron spins<sup>15</sup> is described by the following evident generalization of the Pauli Hamiltonian (4.163),

<sup>12</sup> See, e.g. *Part EM* section 1.3, in particular Eq. (1.54).

<sup>13</sup> Note that the result for  $E_{\text{dir}}$  correctly reflects the basic fact that a charged particle does not interact with itself, even if its wavefunction is quantum-mechanically spread over a finite space volume. Unfortunately, this is not true for some other approximate theories of multiparticle systems—see section 8.4 below.

<sup>14</sup> This traditional terminology reflects the historic fact that the observation of two different hydrogen-like spectra, corresponding to opposite signs in Eq. (8.39), was first taken as an evidence for two different species of <sup>4</sup>He, which were called, respectively, the 'orthohelium' and the 'parahelium'.

<sup>15</sup> As we know from section 6.4, the field also affects the orbital motion of the electrons, so that the simple analysis based on Eq. (8.46) is strictly valid only for the  $s$  excited state ( $l = 0$ , and hence  $m = 0$ ). However, orbital effects of a very weak magnetic field do not affect the triplet level splitting we are analyzing now.

$$\hat{H}_{\text{field}} = -\gamma\hat{\mathbf{s}}_1 \cdot \mathcal{B} - \gamma\hat{\mathbf{s}}_2 \cdot \mathcal{B} \equiv -\gamma\hat{\mathbf{S}} \cdot \mathcal{B}, \quad \text{with } \gamma = \gamma_e \equiv -\frac{e}{m_e} \equiv -\frac{2}{\hbar}\mu_B, \quad (8.46)$$

where

$$\hat{\mathbf{S}} \equiv \hat{\mathbf{s}}_1 + \hat{\mathbf{s}}_2, \quad (8.47)$$

is the operator of the (vector) sum of the system of two spins<sup>16</sup>.

In order to analyze this effect, we need first to make one more detour, to address the general issue of *spin addition*. The main rule<sup>17</sup> here is that in a full analogy with the net spin of a single particle, defined by Eq. (5.170), the net spin operator (8.47) of *any* system of two spins, and its component  $\hat{S}_z$  along an arbitrary axis, obey the same commutation relations (5.168) as the component operators, and hence have properties similar to those expressed by Eqs. (5.169) and (5.175):

$$\begin{aligned} \hat{S}^2|S, M_S\rangle &= \hbar^2 S(S+1)|S, M_S\rangle, \\ \hat{S}_z|S, M_S\rangle &= \hbar M_S|S, M_S\rangle, \quad \text{with } -S \leq M_S \leq +S, \end{aligned} \quad (8.48)$$

where the ket vectors correspond to the coupled basis of joint eigenstates of the operators of  $S^2$  and  $S_z$  (but not necessarily all component operators—see again the Venn shown in figure 5.12 and its discussion, with the replacements  $\mathbf{S}, \mathbf{L} \rightarrow \mathbf{s}_{1,2}$  and  $\mathbf{J} \rightarrow \mathbf{S}$ ). Repeating the discussion of section 5.7 with these replacements, we see that in both coupled and uncoupled bases, the net magnetic number  $M_S$  is simply expressed via those of the components

$$M_S = (m_s)_1 + (m_s)_2. \quad (8.49)$$

However, the net spin quantum number  $S$  (in contrast to the Nature-given spins  $s_{1,2}$  of its elementary components) is not quite certain, and we may immediately say only that it has to obey the following analog of the relation  $|l - s| \leq j \leq l + s$ , discussed in section 5.7:

$$|s_1 - s_2| \leq S \leq s_1 + s_2. \quad (8.50)$$

What exactly  $S$  is (within these limits), depends on the spin state of the system.

For the simplest case of two spin- $1/2$  components, with each  $s = 1/2$  and  $m_s = \pm 1/2$ , Eq. (8.49) gives three possible values of  $M_S$ , equal to 0 and  $\pm 1$ , while Eq. (8.50) limits the possible values of  $S$  to just either 0 or 1. Using the last of Eqs. (8.48), we see that the possible combinations of the quantum numbers are

<sup>16</sup>Note that similarly to Eqs. (8.22) and (8.25), here the uppercase notation of the component spins is replaced with their lowercase notation, to avoid any possibility of their confusion with the total spin of the system.

<sup>17</sup>Since we already know that the spin of a particle is physically nothing more than a (specific) part of its angular momentum, the similarity of the properties (8.48) of the sum (8.47) of spins of different particles to those of the sum (5.170) of different spin components of the same particle is very natural, but still has to be considered as a new law of Nature—confirmed by a vast body of experimental data.

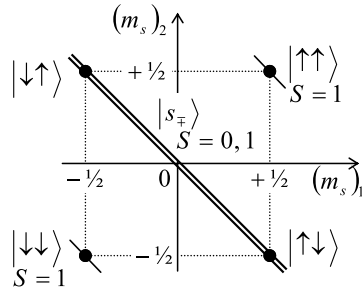


**Figure 8.2.** The ‘rectangular diagram’ showing the relation between the uncoupled-representation states (dots) and the coupled-representation states (straight lines) of a system of two spins- $\frac{1}{2}$ —cf. figure 5.14.

$$\begin{cases} S = 0, \\ M_S = 0, \end{cases} \quad \text{and} \quad \begin{cases} S = 1, \\ M_S = 0, \pm 1. \end{cases} \quad (8.51)$$

It is virtually evident that the singlet spin state  $s_-$  belongs to the first class, while the simple (separable) triplet states  $\uparrow\uparrow$  and  $\downarrow\downarrow$  belong to the second class, with  $M_S = +1$  and  $M_S = -1$ , respectively. However, for the entangled triplet state  $s_+$ , evidently with  $M_S = 0$ , the value of  $S$  is less obvious. Perhaps the easiest way to recover it<sup>18</sup> is to use the ‘rectangular diagram’, similar to that shown in figure 5.14, but redrawn for our case, i.e. with the replacements  $m_l \rightarrow (m_s)_1 = \pm\frac{1}{2}$ ,  $m_s \rightarrow (m_s)_2 = \pm\frac{1}{2}$ —see figure 8.2.

Just as at the addition of angular momenta of a single particle, the top-right and bottom-left corners of this diagram correspond to the factorable triplet states  $\uparrow\uparrow$  and  $\downarrow\downarrow$ , which participate in both the uncoupled-representation and coupled-representation bases, and have the largest value of  $S$ , i.e. 1. However, the entangled states  $s_{\pm}$ , which are linear combinations of the uncoupled-representation states  $\uparrow\downarrow$  and  $\downarrow\uparrow$ , cannot have the same value of  $S$ , so that for the triplet state  $s_+$ ,  $S$  has to take the value different from that (0) of the singlet state, i.e. 1. With that, the first of Eqs. (8.48) gives the following expectation values for the square of the net spin operator:

$$\langle S^2 \rangle = \begin{cases} 2\hbar^2, & \text{for each triplet state,} \\ 0, & \text{for the singlet state.} \end{cases} \quad (8.52)$$

Note that for the entangled triplet state  $s_+$ , whose ket-vector (8.20) is a linear superposition of two kets of states with *opposite* spins, this result is highly counter-intuitive, and shows how careful we should be interpreting quantum entangled states. (As will be discussed in chapter 10, the entanglement brings even more surprises for quantum measurements.)

Now returning for a moment to the particular issue of the magnetic field effect on the spins of  ${}^4\text{He}$  atom’s electrons, directing the axis  $z$  along the field, we may reduce Eq. (8.46) to

<sup>18</sup> Another, somewhat longer but perhaps more prudent way is to directly calculate the expectation values of  $\hat{S}^2$  for the states  $s_{\pm}$ , and then find  $S$  by comparing the results with the first of Eqs. (8.48); it is highly recommended to the reader as a useful exercise.

$$\hat{H}_{\text{field}} = -\gamma_e \hat{S}_z \mathcal{B} \equiv 2\mu_B \mathcal{B} \frac{\hat{S}_z}{\hbar}. \quad (8.53)$$

Since all three triplet states (8.21) are eigenstates, in particular, of the operator  $\hat{S}_z$ , and hence of this Hamiltonian, we may use the second of Eqs. (8.48) to calculate their energy change simply as

$$\Delta E_{\text{field}} = 2\mu_B \mathcal{B} M_S = 2\mu_B \mathcal{B} \times \begin{cases} +1, & \text{for the factorable triplet state } \uparrow \uparrow, \\ 0, & \text{for the entangled triplet state } s_+, \\ -1, & \text{for the factorable triplet state } \downarrow \downarrow. \end{cases} \quad (8.54)$$

This splitting of the ‘orthohelium’ level is schematically shown in figure 8.1b.<sup>19</sup>

### 8.3 Multiparticle systems

Leaving several other problems on two-particle systems for the reader’s exercise, let me proceed to the discussion of systems with  $N > 2$  indistinguishable particles, whose list notably includes atoms, molecules, and condensed-matter systems. In this case, Eq. (8.7) for fermions is generalized as

$$\hat{\mathcal{P}}_{kk'} |\alpha_{-}\rangle = -|\alpha_{-}\rangle, \quad \text{for all } k, k' = 1, 2, \dots, N, \quad (8.55)$$

where the operator  $\hat{\mathcal{P}}_{kk'}$  permutes particles with numbers  $k$  and  $k'$ . As a result, for systems with non-directly-interacting fermions, the Pauli principle forbids any state in which *any* two particles have similar single-particle wavefunctions. Nevertheless, it permits two fermions to have similar *orbital* wavefunctions, provided that their spins are in the singlet state (8.18), because this satisfies the permutation requirement (8.55). This fact has the paramount importance for the ground state of the systems whose Hamiltonians do not depend on spin, because it allows the fermions to be in their orbital single-particle ground states, with two electrons of the spin singlet sharing the same orbital state. Hence, for the limited (but very important!) goal of finding ground-state energies of multi-fermion systems with negligible direct interaction, we may ignore the actual singlet spin structure, and reduce the Pauli exclusion principle to the simple picture of single-particle orbital energy levels, each ‘occupied’ with two fermions.

As a very simple example, let us find the ground energy of five fermions, confined in a hard-wall, cubic-shaped 3D volume of side  $a$ , ignoring their direct interaction. From section 1.7, we know the single-particle energy spectrum of the system:

<sup>19</sup> It is interesting that another very important two-electron system, the hydrogen ( $\text{H}_2$ ) molecule, which was briefly discussed in section 2.6, also has two similarly named forms, *parahydrogen* and *orthohydrogen*. However, their difference is due to two possible (respectively, singlet and triplet) states of the system of two spins of the hydrogen *nuclei* (protons), which are also spin- $1/2$  particles. The resulting energy of the parahydrogen is lower than that of the orthohydrogen by only  $\sim 45$  meV per molecule—the difference comparable with  $k_B T$  at room temperature ( $\sim 26$  meV). As a result, at the ambient conditions, the equilibrium ratio of these two *spin isomers* is close to 3:1. Curiously, the theoretical prediction of this minor effect by W Heisenberg (together with F Hund) in 1927 was cited in his 1932 Nobel Prize award as the most noteworthy application of quantum theory.

$$\varepsilon_{n_x, n_y, n_z} = \varepsilon_0(n_x^2 + n_y^2 + n_z^2), \quad \text{with} \quad \varepsilon_0 \equiv \frac{\pi^2 \hbar^2}{2ma^2}, \quad \text{and} \quad n_x, n_y, n_z = 1, 2, \dots \quad (8.56)$$

so that the lowest-energy states are:

- one ground state with  $\{n_x, n_y, n_z\} = \{1, 1, 1\}$ , and energy  $\varepsilon_{111} = (1^2 + 1^2 + 1^2)\varepsilon_0 = 3\varepsilon_0$ , and
- three excited states, with  $\{n_x, n_y, n_z\}$  equal to  $\{2, 1, 1\}$ ,  $\{1, 2, 1\}$ , and  $\{1, 1, 2\}$ , with equal energies  $\varepsilon_{211} = \varepsilon_{121} = \varepsilon_{112} = (2^2 + 1^2 + 1^2)\varepsilon_0 = 6\varepsilon_0$ .

According to the above simple formulation of the Pauli principle, each of these orbital energy levels can accommodate up to two fermions. Hence the lowest-energy (ground) state of the five-fermion system is achieved by placing two of them on the ground level  $\varepsilon_{111} = 3\varepsilon_0$ , and the remaining three particles, in any degenerate ‘excited’ states of energy  $6\varepsilon_0$ , so that the ground-state energy of the system is

$$E_g = 2 \times 3\varepsilon_0 + 3 \times 6\varepsilon_0 \equiv 24\varepsilon_0 \equiv \frac{12\pi^2 \hbar^2}{ma^2}. \quad (8.57)$$

Moreover, in many cases a relatively weak interaction between fermions does not blow up such a simple quantum state classification scheme qualitatively, and the Pauli principle allows tracing the order of single-particle state filling. This is exactly the simple approach that has been used at our discussion of atoms in section 3.7. Unfortunately, it does not allow for a more specific characterization of the ground states of most atoms, in particular the evaluation of the corresponding values of the quantum numbers  $S$ ,  $L$ , and  $J$  that characterize the net angular momenta of the atom, and hence its response to external magnetic field. These numbers are defined by relations similar to Eqs. (8.48), for the vector-operators of total angular momenta:

$$\hat{\mathbf{S}} \equiv \sum_{k=1}^N \hat{\mathbf{s}}_k, \quad \hat{\mathbf{L}} \equiv \sum_{k=1}^N \hat{\mathbf{l}}_k, \quad \hat{\mathbf{J}} \equiv \sum_{k=1}^N \hat{\mathbf{j}}_k; \quad (8.58)$$

note that these definitions are consistent with Eq. (5.170) applied both to the angular momenta  $\mathbf{s}_k$ ,  $\mathbf{l}_k$ , and  $\mathbf{j}_k$  of each particle, and to the full vectors  $\mathbf{S}$ ,  $\mathbf{L}$ , and  $\mathbf{J}$ . When the numbers  $S$ ,  $L$ , and  $J$  for a state are known, they are traditionally recorded in the form of the so-called *Russell–Saunders symbols*<sup>20</sup>:

$${}^{2S+1}\mathcal{L}_J, \quad (8.59)$$

where  $S$  and  $J$  are the corresponding values of these quantum numbers, while  $\mathcal{L}$  is a capital *letter*, encoding the quantum number  $L$  via the same spectroscopic notation as for single particles (see section 3.6):  $\mathcal{L} = S$  for  $L = 0$ ,  $\mathcal{L} = P$  for  $L = 1$ ,  $\mathcal{L} = D$  for  $L = 2$ , etc. (The reason why the front superscript of the Russel–Saunders symbol lists  $2S + 1$  rather than  $S$ , is that according to the last of Eqs. (8.48), it shows the number

<sup>20</sup> Named after H Russell and F Saunders, whose pioneering (circa 1925) processing of experimental spectral-line data has established the very idea of vector addition of electron spins, described by the first of Eqs. (8.58).



of possible values of the quantum number  $M_S$ , which characterizes the state's spin degeneracy, and is called its *multiplicity*.)

For example, for the simplest, hydrogen atom ( $Z = 1$ ), with its single electron in the ground  $1s$  state,  $L = l = 0$ ,  $S = s = 1/2$ , and  $J = S = 1/2$ , so that its Russell–Saunders symbol is  $2S_{1/2}$ . Next, the discussion of the helium atom ( $Z = 2$ ) in the previous section has shown that in its ground state  $L = 0$  (because of the  $1s$  orbital state of both electrons), and  $S = 0$  (because of the singlet spin state), so that the total angular momentum also vanishes:  $J = 0$ . As a result, the Russell–Saunders symbol is  $1S_0$ . The structure of the next atom, lithium ( $Z = 3$ ) is also easy to predict, because, as was discussed in section 3.7, its ground-state electron configuration is  $1s^2 2s^1$ , i.e. includes two electrons in the 'helium shell', i.e. on the  $1s$  orbitals (now we know that they are actually in a singlet spin state), and one electron in the  $2s$  state, of much higher energy, also with zero orbital moment,  $l = 0$ . As a result, the total  $L$  in this state is evidently equal to 0, and  $S$  is equal to  $1/2$ , so that  $J = 1/2$ , meaning that the Russell–Saunders symbol of lithium is  $2P_{1/2}$ . Even the next atom, beryllium ( $Z = 4$ ), with the ground-state configuration  $1s^2 2s^2$ , is readily predictable, because none of its electrons has orbital momentum, giving  $L = 0$ . Also, each electron pair is in the singlet spin state, i.e. we have  $S = 0$ , so that  $J = 0$ —the quantum number set described by the Russell–Saunders symbol  $1S_0$ —just as for helium.

However, for the next, boron atom ( $Z = 5$ ), with its ground-state electron configuration  $1s^2 2s^2 2p^1$  (see, e.g. figure 3.24), there is no obvious way to predict the result. Indeed, this atom has two pairs of electrons, with opposite spins, on its two lowest  $s$ -orbitals, giving zero contributions to the net  $S$ ,  $L$ , and  $J$ . Hence these total quantum numbers may be only contributed by the last, fifth electron with  $s = 1/2$  and  $l = 1$ , giving  $S = 1/2$ ,  $L = 1$ . As was discussed in section 5.7 for the single-particle case, the vector addition of the angular momenta  $\mathbf{S}$  and  $\mathbf{L}$  enables two values rather than one of the quantum number  $J$ : either  $L + S = 3/2$ , or  $L - S = 1/2$ . Experiment shows that the difference between the energies of these two states is very small ( $\sim 2$  meV), so that at room temperature they are both occupied, with the genuine ground state having  $J = 1/2$ , so that its Russell–Saunders symbol is  $2P_{1/2}$ .

Such energy differences, which become larger for heavier atoms, are determined both by the Coulomb and spin–orbit<sup>21</sup> interactions between the electrons. Their quantitative analysis is rather involved (see below), but the results tend to follow simple phenomenological *Hund rules*, with the following hierarchy:

*Rule 1.* For a given electron configuration, the ground state has the *largest* possible  $S$ , and hence the largest multiplicity.

*Rule 2.* For a given  $S$ , the ground state has the *largest* possible  $L$ .

*Rule 3.* For given  $S$  and  $L$ ,  $J$  has its *smallest* possible value,  $|L - S|$ , if the given sub-shell  $\{n, l\}$  is filled not more than by half, while in the opposite case,  $J$  has its *largest* possible value,  $L + S$ .

<sup>21</sup> In light atoms, the spin–orbit interaction is so weak that it may be reasonably well described as interaction of the total momenta  $\mathbf{L}$  and  $\mathbf{S}$  of the system—the so-called *LS* (or 'Russell–Saunders') *coupling*. On the other hand, in very heavy atoms, the interaction is effectively between the net momenta  $\mathbf{j}_k = \mathbf{l}_k + \mathbf{s}_k$  of the individual electrons—the so-called *jj coupling*. This is the reason why in such atoms the Hund's Rule 3 may be violated.

Let us see how these rules work for the boron atom. For it, the Hund Rules 1 and 2 are satisfied automatically, while the sub-shell  $\{n = 2, l = 1\}$ , which can house up to  $(2l + 1)s = 6$  electrons, is filled less than by half with just one  $2p$  electron. As a result, the Hund Rule 3 predicts the ground state's value  $J = 1/2$ , in agreement with experiment. Generally, for lighter atoms the Hund rules are well obeyed. However, the lower down the Hund rule hierarchy, the less 'powerful' the rules are, i.e. in more heavier atoms they are violated.

Now let us discuss possible approaches to a quantitative theory of multiparticle systems—not only atoms. As was discussed in section 8.1, if fermions do not interact directly, the stationary states of the system have to be the antisymmetric eigenstates of the permutation operator, i.e. satisfy Eq. (8.55). In order to understand how such states may be formed from the single-electron ones, let us return for a minute to the case of two electrons, and rewrite Eq. (8.11) in the following compact form:

$$\begin{aligned}
 & \begin{array}{ccc} & \text{state 1} & \text{state 2} \\ & \downarrow & \downarrow \\ & & \end{array} & (8.60a) \\
 |\alpha_{-}\rangle \equiv \frac{1}{\sqrt{2}} (|\beta\rangle \otimes |\beta'\rangle - |\beta'\rangle \otimes |\beta\rangle) & \equiv \frac{1}{\sqrt{2}} \left[ \begin{array}{cc} |\beta\rangle & |\beta'\rangle \\ |\beta\rangle & |\beta'\rangle \end{array} \right] \begin{array}{l} \leftarrow \text{particle number 1,} \\ \leftarrow \text{particle number 2,} \end{array}
 \end{aligned}$$

where the direct product signs are just implied. In this way, the Pauli principle is mapped on the well-known property of matrix determinants: if any of two columns of a matrix coincide, its determinant vanishes. This *Slater determinant* approach<sup>22</sup> may be readily generalized to  $N$  fermions in  $N$  (not necessarily the lowest) single-particle states  $\beta, \beta', \beta'',$  etc:

$$|\alpha_{-}\rangle = \frac{1}{(N!)^{1/2}} \underbrace{\left[ \begin{array}{cccc} \text{state list } \rightarrow \\ |\beta\rangle & |\beta'\rangle & |\beta''\rangle & \dots \\ |\beta\rangle & |\beta'\rangle & |\beta''\rangle & \dots \\ |\beta\rangle & |\beta'\rangle & |\beta''\rangle & \dots \\ \dots & \dots & \dots & \dots \end{array} \right]}_N \left. \begin{array}{l} \text{particle} \\ \text{list} \\ \downarrow \end{array} \right\} N \quad (8.60b)$$

Even though the Slater determinant form is extremely nice and compact (in comparison with direct writing of a sum of  $N!$  products, each of  $N$  ket factors), there are two major problems with using it for practical calculations:

(i) For the calculation of any bra-ket product (say, within the perturbation theory) we still need to spell out each bra- and ket-vector as a sum of component terms. Even for a limited number of electrons (say  $N \sim 10^2$  in a typical atom), the number  $N! \sim 10^{160}$  of terms in such a sum is impracticably large for any analytical or numerical calculation.

(ii) In the case of interacting fermions, the Slater determinant does not describe the eigenvectors of the system; rather the stationary state is a *superposition* of such

<sup>22</sup>It was suggested in 1929 by J Slater.

basis functions, i.e. the Slater determinants—each for a specific selection of  $N$  states from the general set of single-particle states—that is generally larger than  $N$ .

For atoms and simple molecules, whose filled-shell electrons may be excluded from an explicit analysis (by describing their effects, approximately, with effective *pseudo-potentials*), the effective number  $N$  may be reduced to a smaller number  $N_{\text{ef}}$  of the order of 10, so that  $N_{\text{ef}}! < 10^6$ , and the Slater determinants may be used for numerical calculations—for example, in the Hartree–Fock theory—see the next section. However, for condensed-matter systems, such as metals and semiconductors, with the number of free electrons is of the order of  $10^{23}$  per  $\text{cm}^3$ , this approach is generally unacceptable, though with some smart tricks (such as using crystal periodicity) it may be still used for some approximate (also numerical) calculations.

These challenges make the development of a more general theory that would not use particle numbers (which are superficial for indistinguishable particles to start with) a must for getting any final analytical results for multiparticle systems. The most effective formalism for this purpose, that avoids particle numbering at all, is called the *second quantization*<sup>23</sup>. Actually, we have already discussed a particular version of this formalism, for the case of 1D harmonic oscillator, in section 5.4. As a reminder, after the definition (5.65) of the ‘creation’ and ‘annihilation’ operators via those of the particle’s coordinate and momentum, we have derived their key properties (5.89),

$$\hat{a}|n\rangle = n^{1/2}|n-1\rangle, \quad \hat{a}^\dagger|n\rangle = (n+1)^{1/2}|n+1\rangle, \quad (8.61)$$

where  $n$  were the stationary (Fock) states of the oscillator. This property allows an interpretation of the operators’ actions as the creation/annihilation of a single *excitation* with the energy  $\hbar\omega_0$ —thus justifying the operator names. In the next chapter, we will show that such an excitation of an electromagnetic field mode may be interpreted as a massless *boson* with  $s = 1$ , called the *photon*.

In order to generalize this approach to *arbitrary* bosons, not appealing to a specific system, we may use relations similar to Eq. (8.61) to *define* the creation and annihilation operators. The definitions look simple in the language of the so-called *Dirac states*, described by ket-vectors

$$|N_1, N_2, \dots, N_j, \dots\rangle, \quad (8.62)$$

where  $N_j$  is the state *occupancy*, i.e. the number of bosons in the single-particle state  $j$ . Let me emphasize that here the indices  $1, 2, \dots, j, \dots$  number single-particle *states* (including their spin parts) rather than *particles*. Thus the very notion of an individual particle’s number is completely (and for indistinguishable particles, very relevantly) absent from this formalism. Generally, the set of single-particle

---

<sup>23</sup> It was invented (first for photons and then for arbitrary bosons) by P Dirac in 1927, and then modified in 1928 for fermions by E Wigner and P Jordan. Note that the term ‘second quantization’ is rather misleading for the non-relativistic applications we are discussing here, but finds certain justification in the quantum field theory.

states participating in the Dirac state may be selected in an arbitrary way, provided that it is full and orthonormal in the sense

$$\langle N'_1, N'_2, \dots, N'_j, \dots | N_1, N_2, \dots, N_j, \dots \rangle = \delta_{N_1 N'_1} \delta_{N_2 N'_2} \dots \delta_{N_j N'_j} \dots, \quad (8.63)$$

though for systems of non- (or weakly) interacting bosons, using the stationary states of individual particles in the system under analysis is almost always the best choice.

Now we can define the *particle annihilation operator* as follows:

$$\hat{a}_j |N_1, N_2, \dots, N_j, \dots\rangle \equiv N_j^{1/2} |N_1, N_2, \dots, N_j - 1, \dots\rangle. \quad (8.64)$$

Note that the pre-ket coefficient, similar to that in the first of Eqs. (8.61), guarantees that an attempt to annihilate a particle in an unpopulated state gives the non-existing ('null') state:

$$\hat{a}_j |N_1, N_2, \dots, 0_j, \dots\rangle = 0, \quad (8.65)$$

where the symbol  $0_j$  means zero occupancy of the  $j$ th state. According to Eq. (8.63), an alternative way to write Eq. (8.64) is

$$\langle N'_1, N'_2, \dots, N'_j, \dots | \hat{a}_j |N_1, N_2, \dots, N_j, \dots\rangle = N_j^{1/2} \delta_{N_1 N'_1} \delta_{N_2 N'_2} \dots \delta_{N_j, N_j-1} \dots \quad (8.66)$$

According to the general Eq. (4.65), the matrix element of the Hermitian conjugate operator  $\hat{a}_j^\dagger$  is

$$\begin{aligned} & \langle N'_1, N'_2, \dots, N'_j, \dots | \hat{a}_j^\dagger |N_1, N_2, \dots, N_j, \dots\rangle \\ &= \langle N_1, N_2, \dots, N_j, \dots | \hat{a}_j |N'_1, N'_2, \dots, N'_j, \dots\rangle^* \\ &= \langle N_1, N_2, \dots, N_j, \dots | (N'_j)^{1/2} |N'_1, N'_2, \dots, N'_j - 1, \dots\rangle \\ &= (N'_j)^{1/2} \delta_{N_1 N'_1} \delta_{N_2 N'_2} \dots \delta_{N_j, N'_j-1} \dots \\ &= (N_j + 1)^{1/2} \delta_{N_1 N'_1} \delta_{N_2 N'_2} \dots \delta_{N_j+1, N'_j} \dots, \end{aligned} \quad (8.67)$$

meaning that

$$\hat{a}_j^\dagger |N_1, N_2, \dots, N_j, \dots\rangle = (N_j + 1)^{1/2} |N_1, N_2, \dots, N_j + 1, \dots\rangle, \quad (8.68)$$

in the total compliance with the second of Eqs. (8.61). In particular, this *particle creation operator* allows the description of the generation of a single particle from the *vacuum* (not null!) *state*  $|0, 0, \dots\rangle$ :

$$\hat{a}_j^\dagger |0, 0, \dots, 0_j, \dots, 0\rangle = |0, 0, \dots, 1_j, \dots, 0\rangle, \quad (8.69)$$

and hence a product of such operators may create, from the vacuum, a multiparticle state with an arbitrary set of occupancies<sup>24</sup>:

$$\underbrace{\hat{a}_1^\dagger \hat{a}_1^\dagger \dots \hat{a}_1^\dagger}_{N_1 \text{ times}} \underbrace{\hat{a}_2^\dagger \hat{a}_2^\dagger \dots \hat{a}_2^\dagger}_{N_2 \text{ times}} \dots |0, 0, \dots\rangle = (N_1! N_2! \dots)^{1/2} |N_1, N_2, \dots\rangle. \quad (8.70)$$

Next, combining Eqs. (8.64) and (8.68), we get

$$\hat{a}_j^\dagger \hat{a}_j |N_1, N_2, \dots, N_j, \dots\rangle = N_j |N_1, N_2, \dots, N_j, \dots\rangle, \quad (8.71)$$

so that, just as for the particular case of harmonic oscillator excitations, the operator

$$\hat{N}_j \equiv \hat{a}_j^\dagger \hat{a}_j \quad (8.72)$$

‘counts’ the number of particles in the  $j$ th single-particle state, while preserving the whole multiparticle state. Acting on a state by the creation–annihilation operators in the reverse order, we get

$$\hat{a}_j \hat{a}_j^\dagger |N_1, N_2, \dots, N_j, \dots\rangle = (N_j + 1) |N_1, N_2, \dots, N_j, \dots\rangle. \quad (8.73)$$

Eqs. (8.71) and (8.73) show that for *any* state of a multiparticle system (which always may be represented as a linear superposition of Dirac states with all possible sets of numbers  $N_j$ ), we may write

$$\hat{a}_j \hat{a}_j^\dagger - \hat{a}_j^\dagger \hat{a}_j \equiv [\hat{a}_j, \hat{a}_j^\dagger] = \hat{I}, \quad (8.74)$$

again in agreement with what we had for the 1D oscillator—cf. Eq. (5.68). According to Eqs. (8.63), (8.64) and (8.68), the creation and annihilation operators corresponding to different single-particle states do commute, so that Eq. (8.74) may be generalized as

$$[\hat{a}_j, \hat{a}_{j'}^\dagger] = \hat{I} \delta_{jj'}, \quad (8.75)$$

while the similar operators commute, regardless of which states do they act upon:

$$[\hat{a}_j^\dagger, \hat{a}_{j'}^\dagger] = [\hat{a}_j, \hat{a}_{j'}] = \hat{0}. \quad (8.76)$$

As was mentioned earlier, a major challenge in the Dirac approach is to rewrite the Hamiltonian of a multiparticle system, that naturally carries particle numbers  $k$  (see, e.g. Eq. (8.22) for  $k = 1, 2$ ), in the second quantization language, in which there are not these numbers. Let us start with *single-particle* components of such Hamiltonians, i.e. operators of the type

$$\hat{F} = \sum_{k=1}^N \hat{f}_k. \quad (8.77)$$

<sup>24</sup> The resulting Dirac state is *not* an eigenstate of every multiparticle Hamiltonian. However, we will see below that for a set of non-interacting particles it *is* a stationary state, so that the full set of such states may be used as a good basis in perturbation theories of systems of weakly interacting particles.

where all  $N$  operators  $\hat{f}_k$  are similar, besides that each of them acts on one specific ( $k$ th) particle, and  $N$  is the total number of particles in the system, which is evidently equal to the sum of single-particle state occupancies:

$$N = \sum_j N_j. \quad (8.78)$$

The most important examples of such operators are the kinetic energy of  $N$  similar single particles, and their potential energy in an external field:

$$\hat{T} = \sum_{k=1}^N \frac{\hat{p}_k^2}{2m}, \quad \hat{U} = \sum_{k=1}^N \hat{u}(\mathbf{r}_k). \quad (8.79)$$

For bosons, instead of the Slater determinant (8.60), we have to write a similar expression, but without the sign alternation at permutations:

$$|N_1, \dots, N_j, \dots\rangle = \left( \frac{N_1! \dots N_j! \dots}{N!} \right)^{1/2} \sum_P \left| \underbrace{\dots \beta \beta' \beta'' \dots}_{N \text{ operands}} \right\rangle, \quad (8.80)$$

sometimes called the *permanent*. Note again that the left-hand side of this relation is written in the Dirac notation (that does not use particle numbering), while on its right-hand side, just in relations of sections 8.1 and 8.2, the particle numbers are coded with the positions of the single-particle states inside the ket-vectors, and the sum is over all different permutations of the states in the ket—cf. Eq. (8.10). (According to the basic combinatorics<sup>25</sup>, there are  $N!/(N_1! \dots N_j! \dots)$  such permutations, so that the front coefficient in Eq. (8.80) ensures the normalization of the Dirac state, provided that the single-particle states  $\beta, \beta', \dots$  are normalized.) Let us use Eq. (8.80) to spell out the following matrix element for a system with  $(N - 1)$  particles:

$$\begin{aligned} & \langle \dots N_j, \dots N_{j'} - 1, \dots | \hat{F} | \dots N_j - 1, \dots N_{j'}, \dots \rangle \\ &= \frac{N_1! \dots (N_j - 1)! \dots (N_{j'} - 1)! \dots}{(N - 1)!} (N_j N_{j'})^{1/2} \\ & \times \sum_{P \langle N-1 |} \sum_{P \langle N-1 |} \langle \dots \beta \beta' \beta'' \dots | \sum_{k=1}^{N-1} \hat{f}_k | \dots \beta \beta' \beta'' \dots \rangle, \end{aligned} \quad (8.81)$$

where all non-specified occupation numbers in the corresponding positions of the bra- and ket-vectors are equal to each other. Each single-particle operator  $\hat{f}_k$ , participating in the operator sum, acts on the bra- and ket-vectors of states only in one ( $k$ th) position, giving the result, which does not depend on the position number:

<sup>25</sup> See, e.g. Eq. (A.6).

$$\langle \beta_j |_{\text{in } k^{\text{th}} \text{ position}} \hat{f}_k | \beta_{j'} \rangle_{\text{in } k^{\text{th}} \text{ position}} = \langle \beta_j | \hat{f} | \beta_{j'} \rangle \equiv f_{jj'}. \quad (8.82)$$

Since in both permutation sets participating in Eq. (8.81), with  $(N - 1)$  state vectors each, all positions are equivalent, we can fix the position (say, take the first one) and replace the sum over  $k$  with the multiplication by of the bracket by  $(N - 1)$ . The fraction of permutations with the necessary bra-vector (with number  $j$ ) in that position is  $N_j/(N - 1)$ , while that with the necessary ket-vector (with number  $j'$ ) in the same position is  $N_{j'}/(N - 1)$ . As a result, the permutation sum in Eq. (8.81) reduces to

$$(N - 1) \frac{N_j}{N - 1} \frac{N_{j'}}{N - 1} f_{jj'} \sum_{P(N-2)} \sum_{P(N-2)} \langle \dots \beta \beta' \beta'' \dots | \dots \beta \beta' \beta'' \dots \rangle, \quad (8.83)$$

where our specific position  $k$  is now excluded from both the bra- and ket-vector permutations. Each of these permutations now includes only  $(N_j - 1)$  states  $j$  and  $(N_{j'} - 1)$  states  $j'$ , so that, using the state orthonormality, we finally arrive at a very simple result:

$$\begin{aligned} & \langle \dots N_j, \dots N_{j'} - 1, \dots | \hat{F} | \dots N_j - 1, \dots N_{j'}, \dots \rangle \\ &= \frac{N_1! \dots (N_j - 1)! \dots (N_{j'} - 1)! \dots}{(N - 1)!} (N_j N_{j'})^{1/2} (N - 1) \\ & \times \frac{N_j}{N - 1} \frac{N_{j'}}{N - 1} f_{jj'} \frac{(N - 2)!}{N_1! \dots (N_j - 1)! \dots (N_{j'} - 1)! \dots} \equiv (N_j N_{j'})^{1/2} f_{jj'}. \end{aligned} \quad (8.84)$$

On the other hand, let us calculate matrix elements of the following operator:

$$\sum_{j,j'} f_{jj'} \hat{a}_j^\dagger \hat{a}_{j'}. \quad (8.85)$$

A direct application of Eqs. (8.64) and (8.68) shows that the only nonvanishing of the elements are

$$\langle \dots N_j, \dots N_{j'} - 1, \dots | f_{jj'} \hat{a}_j^\dagger \hat{a}_{j'} | \dots N_j - 1, \dots, N_{j'}, \dots \rangle = (N_j N_{j'})^{1/2} f_{jj'}. \quad (8.86)$$

But this is exactly the last form of Eq. (8.84), so that in the basis of Dirac states, the operator (8.77) may be represented as

$$\hat{F} = \sum_{j,j'} f_{jj'} \hat{a}_j^\dagger \hat{a}_{j'}. \quad (8.87)$$

This beautifully simple equation is the key formula of the second quantization theory, and is essentially the Dirac-language analog of Eq. (4.59) of the single-particle quantum mechanics. Each term of the sum (8.87) may be described by a very simple mnemonic rule: for each pair of single-particle states  $j$  and  $j'$ , kill a particle in the state  $j'$ , create one in the state  $j$ , and weigh the result with the corresponding

single-particle matrix element. One of corollaries of Eq. (8.87) is that the expectation value of an operator whose eigenstates coincide with the Dirac states, is

$$\langle F \rangle \equiv \langle \dots N_j, \dots | \hat{F} | \dots N_j, \dots \rangle = \sum_j f_{jj} N_j, \quad (8.88)$$

with an evident physical interpretation as the sum of single-particle expectation values over all states, weighed by the occupancy of each state.

Proceeding to *fermions*, which have to obey the Pauli principle, we immediately notice that any occupation number  $N_j$  may only take two values, 0 or 1. In order to account for that, and also make the key relation (8.87) valid for fermions as well, the creation–annihilation operators are now defined by the following relations:

$$\begin{aligned} \hat{a}_j |N_1, N_2, \dots, 0_j, \dots\rangle &= 0, \\ \hat{a}_j |N_1, N_2, \dots, 1_j, \dots\rangle &= (-1)^{\Sigma(1,j-1)} |N_1, N_2, \dots, 0_j, \dots\rangle, \end{aligned} \quad (8.89)$$

$$\begin{aligned} \hat{a}_j^\dagger |N_1, N_2, \dots, 0_j, \dots\rangle &= (-1)^{\Sigma(1,j-1)} |N_1, N_2, \dots, 1_j, \dots\rangle, \\ \hat{a}_j^\dagger |N_1, N_2, \dots, 1_j, \dots\rangle &= 0, \end{aligned} \quad (8.90)$$

where the symbol  $\Sigma(J, J')$  means the sum of all occupancy numbers in the states with numbers from  $J$  to  $J'$ , including the border points:

$$\Sigma(J, J') \equiv \sum_{j=J}^{J'} N_j, \quad (8.91)$$

so that the sum participating in Eqs. (8.89) and (8.90) is the total occupancy of all states with the numbers below  $j$ . (The states are supposed to be numbered in a fixed albeit arbitrary order.) As a result, these relations may be conveniently summarized in the following verbal form: if an operator replaces the  $j$ th state's occupancy with the opposite one (either 1 with 0, or vice versa), it also changes the sign before the result if (and only if) the total number of particles in the states with  $j' < j$  is odd.

Let us use this (perhaps somewhat counter-intuitive) sign alternation rule to spell out the ket-vector  $|11\rangle$  of a completely filled two-state system, formed from the vacuum state  $|00\rangle$  in two different ways. If we start from creating a fermion in the state 1, we get

$$\begin{aligned} \hat{a}_1^\dagger |0, 0\rangle &= (-1)^0 |1, 0\rangle \equiv |1, 0\rangle, \\ \hat{a}_2^\dagger \hat{a}_1^\dagger |0, 0\rangle &= \hat{a}_2^\dagger |1, 0\rangle = (-1)^1 |1, 1\rangle \equiv -|1, 1\rangle, \end{aligned} \quad (8.92a)$$

while if the operator order is different, the result is

$$\begin{aligned} \hat{a}_2^\dagger |0, 0\rangle &= (-1)^0 |0, 1\rangle \equiv |0, 1\rangle, \\ \hat{a}_1^\dagger \hat{a}_2^\dagger |0, 0\rangle &= \hat{a}_1^\dagger |0, 1\rangle = (-1)^0 |1, 1\rangle \equiv |1, 1\rangle, \end{aligned} \quad (8.92b)$$



so that

$$(\hat{a}_1^\dagger \hat{a}_2^\dagger + \hat{a}_2^\dagger \hat{a}_1^\dagger)|0, 0\rangle = 0. \quad (8.93)$$

Since the action of any of these operator products on any initial state rather than the vacuum one also gives the null ket, we can write the following operator equality:

$$\hat{a}_1^\dagger \hat{a}_2^\dagger + \hat{a}_2^\dagger \hat{a}_1^\dagger \equiv \{\hat{a}_1^\dagger, \hat{a}_2^\dagger\} = \hat{0}. \quad (8.94)$$

It is straightforward to check that this result is valid for the Dirac vector of an arbitrary length, and does not depend on the occupancy of other states, so that we can always write

$$\{\hat{a}_j^\dagger, \hat{a}_{j'}^\dagger\} = \{\hat{a}_j, \hat{a}_{j'}\} = \hat{0}; \quad (8.95)$$

these equalities hold for  $j = j'$  as well. On the other hand, an absolutely similar calculation shows that the mixed creation–annihilation commutators do depend on whether the states are different or not<sup>26</sup>:

$$\{\hat{a}_j, \hat{a}_{j'}^\dagger\} = \hat{I}\delta_{jj'}. \quad (8.96)$$

These equations look very much like Eqs. (8.75) and (8.76) for bosons, ‘only’ with the replacement of commutators with anticommutators. Since the core laws of quantum mechanics, including the operator compatibility (section 4.5) and the Heisenberg equation (4.199) of operator evolution in time, involve commutators rather than anticommutators, one might think that all the behavior of bosonic and fermionic multiparticle systems should be dramatically different. However, the difference is not as huge as one could expect; indeed, a straightforward check shows that the sign factors in Eqs. (8.89) and (8.90) just compensate those in the Slater determinant, and thus make the key relation (8.87) valid for the fermions as well. (Indeed, this is the very goal of the introduction of these factors.)

To illustrate this fact on the simplest example, let us examine what the second quantization formalism says about the dynamics of non-interacting particles in the system whose single-particle properties we have discussed repeatedly, namely two nearly-similar potential wells, coupled by tunneling through the separating potential barrier—see, e.g. figures 2.21 or 7.4. If the coupling is so small that the states localized in the wells are only weakly perturbed, then in the basis of these states, the single-particle Hamiltonian of the system may be represented by the  $2 \times 2$  matrix (5.3). With the energy reference selected at the middle between the energies of unperturbed states, the coefficient  $b$  vanishes, this matrix is reduced to

$$\mathbf{h} = \mathbf{c} \cdot \boldsymbol{\sigma} \equiv \begin{pmatrix} c_z & c_- \\ c_+ & -c_z \end{pmatrix}, \quad \text{with } c_{\pm} \equiv c_x \pm ic_y, \quad (8.97)$$

<sup>26</sup>A by-product of this calculation is a proof that the operator defined by Eq. (8.72) counts the number of particles  $N_j$  (now equal to either 1 or 0), just as it does for bosons.

and its eigenvalues to

$$\varepsilon_{\pm} = \pm c, \quad c \equiv |\mathbf{c}| \equiv (c_x^2 + c_y^2 + c_z^2)^{1/2}. \quad (8.98)$$

Now following the recipe (8.87), we can use Eq. (8.97) to represent the Hamiltonian of the whole system of particles in terms of the creation–annihilation operators:

$$\hat{H} = c_z \hat{a}_1^\dagger \hat{a}_1 + c_- \hat{a}_1^\dagger \hat{a}_2 + c_+ \hat{a}_2^\dagger \hat{a}_1 - c_z \hat{a}_2^\dagger \hat{a}_2, \quad (8.99)$$

where  $\hat{a}_{1,2}^\dagger$  and  $\hat{a}_{1,2}$  are the operators of creation and annihilation of a particle in the corresponding *potential well*. (Again, in the second quantization approach the *particles* are not numbered at all!) As Eq. (8.72) shows, the first and the last terms of the right-hand side of Eq. (8.99) describe the particle energies  $\varepsilon_{1,2} = \pm c_z$  in uncoupled wells,

$$c_z \hat{a}_1^\dagger \hat{a}_1 = c_z \hat{N}_1 \equiv \varepsilon_1 \hat{N}_1, \quad -c_z \hat{a}_2^\dagger \hat{a}_2 = -c_z \hat{N}_2 \equiv \varepsilon_2 \hat{N}_2, \quad (8.100)$$

while the sum of the middle two terms is the second-quantization description of tunneling between the wells.

Now we can use the general Eq. (4.199) of the Heisenberg picture to spell out the equations of motion of the creation–annihilation operators. For example,

$$i\hbar \dot{\hat{a}}_1 = [\hat{a}_1, \hat{H}] = c_z [\hat{a}_1, \hat{a}_1^\dagger \hat{a}_1] + c_- [\hat{a}_1, \hat{a}_1^\dagger \hat{a}_2] + c_+ [\hat{a}_1, \hat{a}_2^\dagger \hat{a}_1] - c_z [\hat{a}_1, \hat{a}_2^\dagger \hat{a}_2]. \quad (8.101)$$

Since the Bose and Fermi operators satisfy different commutation relations, one could expect the right hand part of this equation to be different for bosons and fermions. However, it is not so. Indeed, all commutators on the right-hand side of Eq. (8.101) have the following form:

$$[\hat{a}_j, \hat{a}_{j'}^\dagger \hat{a}_{j''}] \equiv \hat{a}_j \hat{a}_j^\dagger \hat{a}_{j''} - \hat{a}_{j'}^\dagger \hat{a}_{j''} \hat{a}_j. \quad (8.102)$$

According to Eqs. (8.74) and (8.94), the first pair product of the operators may be recast as

$$\hat{a}_j \hat{a}_{j'}^\dagger = \hat{I} \delta_{jj'} \pm \hat{a}_{j'}^\dagger \hat{a}_j, \quad (8.103)$$

where the upper sign pertains to bosons and the lower one to fermions, while according to Eqs. (8.76) and (8.95), the very last pair product is

$$\hat{a}_{j'} \hat{a}_j = \pm \hat{a}_j \hat{a}_{j'}, \quad (8.104)$$

with the same sign convention. Plugging these expressions into Eq. (8.102), we see that regardless of the particle type, we arrive at a universal (and generally very useful) commutation relation

$$[\hat{a}_j, \hat{a}_{j'}^\dagger \hat{a}_{j''}] = \hat{a}_{j''} \delta_{jj'}, \quad (8.105)$$

valid for both bosons and fermions. As a result, the Heisenberg equation of motion for the operator  $\hat{a}_1$ , and the equation for  $\hat{a}_2$  (which may be obtained absolutely similarly), are also universal<sup>27</sup>:

$$\begin{aligned} i\hbar\dot{\hat{a}}_1 &= c_-\hat{a}_1 + c_-\hat{a}_2, \\ i\hbar\dot{\hat{a}}_2 &= c_+\hat{a}_1 - c_-\hat{a}_2. \end{aligned} \quad (8.106)$$

This is a system of two coupled, linear differential equations, which is similar to the equations for the  $c$ -number probability amplitudes of single-particle wavefunctions of a two-level system—see, e.g. Eq. (2.201) and the model solution of problem 4.25. Their general solution is a linear superposition

$$\hat{a}_{1,2}(t) = \sum_{\pm} \hat{\alpha}_{1,2}^{(\pm)} \exp\{\lambda_{\pm}t\}. \quad (8.107)$$

As usual, in order to find the exponents  $\lambda_{\pm}$ , it is sufficient to plug in a particular solution  $\hat{a}_{1,2}(t) = \hat{\alpha}_{1,2} \exp\{\lambda t\}$  into Eq. (8.106) and require that the determinant of the resulting homogeneous, linear system for the ‘coefficients’ (actually, time-independent operators)  $\hat{\alpha}_{1,2}$  equals zero. This gives us the following characteristic equation

$$\begin{vmatrix} c_- - i\hbar\lambda & c_- \\ c_+ & -c_- - i\hbar\lambda \end{vmatrix} = 0, \quad (8.108)$$

with two roots  $\lambda_{\pm} = \pm i\Omega/2$ , where  $\Omega \equiv 2c\hbar$ —cf. Eq. (5.20). Now plugging each of the roots, one by one, into the system of equations for  $\hat{\alpha}_{1,2}$ , we can find these operators, and hence the general solution of system (8.98) for arbitrary initial conditions.

Let us consider the simple case  $c_y = c_z = 0$  (meaning in particular that the wells are exactly aligned, see figure 2.21), so that  $\hbar\Omega/2 \equiv c = c_x$ ; then the solution of Eq. (8.106) is

$$\begin{aligned} \hat{a}_1(t) &= \hat{a}_1(0)\cos\frac{\Omega t}{2} - i\hat{a}_2(0)\sin\frac{\Omega t}{2}, \\ \hat{a}_2(t) &= -i\hat{a}_1(0)\sin\frac{\Omega t}{2} + \hat{a}_2(0)\cos\frac{\Omega t}{2}. \end{aligned} \quad (8.109)$$

Multiplying the first of these relations by its Hermitian conjugate, and ensemble-averaging the result, we get

$$\begin{aligned} \langle N_1 \rangle \equiv \langle \hat{a}_1^\dagger(t)\hat{a}_1(t) \rangle &= \langle \hat{a}_1^\dagger(0)\hat{a}_1(0) \rangle \cos^2\frac{\Omega t}{2} + \langle \hat{a}_2^\dagger(0)\hat{a}_2(0) \rangle \sin^2\frac{\Omega t}{2} \\ &\quad - i\langle \hat{a}_1^\dagger(0)\hat{a}_2(0) + \hat{a}_2^\dagger(0)\hat{a}_1(0) \rangle \sin\frac{\Omega t}{2} \cos\frac{\Omega t}{2}. \end{aligned} \quad (8.110)$$

<sup>27</sup> Equations of motion for the creation operators  $\hat{a}_{1,2}^\dagger$  are just the Hermitian-conjugates of Eqs. (8.106), and do not add any new information about system’s dynamics.

Let the initial state of the system be a Dirac state, i.e. have a definite number of particles in each well; in this case only the two first terms on the right hand side of Eq. (8.110) are different from zero, giving<sup>28</sup>:

$$\langle N_1 \rangle = N_1(0)\cos^2 \frac{\Omega t}{2} + N_2(0)\sin^2 \frac{\Omega t}{2}. \quad (8.111)$$

For one particle, initially placed in either well, this gives us our old result (2.181) describing quantum oscillations of the particle between two wells with the frequency  $\Omega$ . However, Eq. (8.111) is valid for any set of initial occupancies; let us use this fact. For example, starting from two particles, with initially one particle in each well, we get  $\langle N_1 \rangle = 1$ , regardless of time. So, the occupancies do not oscillate, and no experiment may detect the quantum oscillations, though their frequency  $\Omega$  is still formally present in the time evolution equations. This fact may be interpreted as the simultaneous quantum oscillations of two particles between the wells, exactly in anti-phase. For bosons, we can go to even larger occupancies by preparing the system, for example, in the state with  $N_1(0) = N$ ,  $N_2(0) = 0$ . The result (8.111) says that in this case we see that the quantum oscillation amplitude increases  $N$ -fold; this is a particular manifestation of the general fact that bosons can be (and evolve in time) in the same quantum state. On the other hand, for fermions we cannot increase the initial occupancies beyond 1, so that the largest oscillation amplitude we can get is if we initially fill just one well.

The Dirac approach may be readily generalized to more complex systems. For example, Eq. (8.99) implies that an arbitrary system of potential wells with weak tunneling coupling between the adjacent wells may be described by the Hamiltonian

$$\hat{H} = \sum_j \varepsilon_j a_j^\dagger \hat{a}_j + \sum_{\langle j,j' \rangle} \delta_{jj'} a_j^\dagger \hat{a}_{j'} + \text{h.c.}, \quad (8.112)$$

where the symbol  $\langle j,j' \rangle$  means that the second sum is restricted to pairs of next-neighbor wells—see, e.g. Eq. (2.203) and its discussion. Note that this Hamiltonian is still a quadratic form of the creation–annihilation operators, so the Heisenberg-picture equations of motion of these operators are still linear, and its exact solutions, though possibly cumbersome, may be studied in detail. Due to this fact, the Hamiltonian (8.112) is widely used for the study of some phenomena, for example the very interesting *Anderson localization* effects, in which a random distribution of the localized-site energies  $\varepsilon_j$  prevents tunneling particles, within a certain energy range, from spreading to unlimited distances<sup>29</sup>.

## 8.4 Perturbative approaches

The situation becomes much more difficult if we need to account for direct interactions between the particles. Let us assume that the interaction may be reduced to that between their pairs (as is the case at their Coulomb interaction

<sup>28</sup> For the second well's occupancy, the result is complementary,  $N_2(t) = N_1(0)\sin^2 \Omega t + N_2(0)\cos^2 \Omega t$ , giving in particular a good sanity check:  $N_1(t) + N_2(t) = N_1(0) + N_2(0) = \text{const}$ .

<sup>29</sup> For a review of the 1D version of this problem, see, e.g. [1].

and most other interactions<sup>30</sup>), so that it may be described by the following ‘pair-interaction’ Hamiltonian

$$\hat{U}_{\text{int}} = \frac{1}{2} \sum_{\substack{k,k'=1 \\ k \neq k'}}^N \hat{u}_{\text{int}}(\mathbf{r}_k, \mathbf{r}_{k'}), \quad (8.113)$$

with the front factor  $\frac{1}{2}$  compensating the double-counting of each particle pair. The translation of this operator to the second-quantization form may be done absolutely similarly to the derivation of Eq. (8.87), and gives a similar (though naturally more involved) result

$$\hat{U}_{\text{int}} = \frac{1}{2} \sum_{j,j',l,l'} u_{jj',ll'} \hat{a}_j^\dagger \hat{a}_{j'}^\dagger \hat{a}_l \hat{a}_{l'}, \quad (8.114)$$

where the two-particle matrix elements are defined similarly to Eq. (8.82):

$$u_{jj',ll'} \equiv \langle \beta_j \beta_{j'} | \hat{u}_{\text{int}} | \beta_l \beta_{l'} \rangle. \quad (8.115)$$

The only new feature of Eq. (8.114) is a specific order of the indices of the creation operators. Note the mnemonic rule of writing this expression, similar to that for Eq. (8.87): each term corresponds to moving a pair of particles from states  $l$  and  $l'$  to states  $j'$  and  $j$  (in this order!) factored with the corresponding two-particle matrix element (8.115).

However, with the account of such term, the resulting Heisenberg equations of time evolution of the creation/annihilation are nonlinear, so that solving them and calculating observables from the results is usually impossible, at least analytically. The only case when some general results may be obtained is the *weak interaction* limit. In this case the unperturbed Hamiltonian contains only single-particle terms such as (8.79), and we can always (at least conceptually) find such a basis of orthonormal single-particle states  $\beta_j$  in which that Hamiltonian is diagonal in the Dirac representation:

$$\hat{H}^{(0)} = \sum_j \varepsilon_j^{(0)} \hat{a}_j^\dagger \hat{a}_j. \quad (8.116)$$

Now we can use Eq. (6.14), in this basis, to calculate the interaction energy as a first-order perturbation:

$$\begin{aligned} E_{\text{int}}^{(1)} &= \langle N_1, N_2, \dots | \hat{U}_{\text{int}} | N_1, N_2, \dots \rangle \\ &= \frac{1}{2} \langle N_1, N_2, \dots | \sum_{j,j',l,l'} u_{jj',ll'} \hat{a}_j^\dagger \hat{a}_{j'}^\dagger \hat{a}_l \hat{a}_{l'} | N_1, N_2, \dots \rangle \\ &= \frac{1}{2} \sum_{j,j',l,l'} u_{jj',ll'} \langle N_1, N_2, \dots | \hat{a}_j^\dagger \hat{a}_{j'}^\dagger \hat{a}_l \hat{a}_{l'} | N_1, N_2, \dots \rangle. \end{aligned} \quad (8.117)$$

<sup>30</sup> A simple but important example from the condensed matter theory is the so-called *Hubbard model*, in which there may be only two particles on each of localized sites, which strongly interact, with negligible interaction of the particles on different sites—though the next-neighbor sites are still connected by tunneling—as in Eq. (8.112).

Since, according to Eq. (8.63), the Dirac states with different occupancies are orthogonal, the last bracket is different from zero only for three particular subsets of its indices:

(i)  $j \neq j'$ ,  $l = j$ , and  $l' = j'$ . In this case the four-operator product in Eq. (8.117) is equal to  $\hat{a}_j^\dagger \hat{a}_j^\dagger \hat{a}_{j'} \hat{a}_j$ , and applying the commutation rules twice, we can bring it to the so-called *normal ordering*, with each creation operator standing to the right of the corresponding annihilation operator, thus forming the particle number operator (8.72):

$$\hat{a}_j^\dagger \hat{a}_j^\dagger \hat{a}_{j'} \hat{a}_j = \pm \hat{a}_j^\dagger \hat{a}_j^\dagger \hat{a}_{j'} \hat{a}_j = \pm \hat{a}_j^\dagger (\pm \hat{a}_j \hat{a}_j^\dagger) \hat{a}_{j'} = \hat{a}_j^\dagger \hat{a}_j \hat{a}_j^\dagger \hat{a}_{j'} = \hat{N}_j \hat{N}_{j'}, \quad (8.118)$$

with the similar sign of the final result for bosons and fermions.

(ii)  $j \neq j'$ ,  $l = j'$ , and  $l' = j$ . In this case the four-operator product is equal to  $\hat{a}_j^\dagger \hat{a}_j^\dagger \hat{a}_{j'} \hat{a}_{j'}$ , and bringing it to the form  $\hat{N}_j \hat{N}_{j'}$  requires only one commutation:

$$\hat{a}_j^\dagger \hat{a}_j^\dagger \hat{a}_{j'} \hat{a}_{j'} = \hat{a}_j^\dagger (\pm \hat{a}_j \hat{a}_j^\dagger) \hat{a}_{j'} = \pm \hat{a}_j^\dagger \hat{a}_j \hat{a}_j^\dagger \hat{a}_{j'} = \pm \hat{N}_j \hat{N}_{j'}, \quad (8.119)$$

with the upper sign for bosons and the lower sign for fermions.

(iii) All indices equal to each other, giving  $\hat{a}_j^\dagger \hat{a}_j^\dagger \hat{a}_l \hat{a}_l = \hat{a}_j^\dagger \hat{a}_j^\dagger \hat{a}_j \hat{a}_j$ . For fermions, such operator (that ‘tries’ to create or to kill two particles in a row, in the same state) immediately gives the null vector. In the case of bosons, we may use Eq. (8.74) to commute the internal pair of operators, getting

$$\hat{a}_j^\dagger \hat{a}_j^\dagger \hat{a}_j \hat{a}_j = \hat{a}_j^\dagger (\hat{a}_j \hat{a}_j^\dagger - \hat{I}) \hat{a}_j = \hat{N}_j (\hat{N}_j - \hat{I}). \quad (8.120)$$

Note, however, that this expression formally covers the fermion case as well (always giving zero). As a result, Eq. (8.117) may be rewritten in the following universal form:

$$E_{\text{int}}^{(1)} = \frac{1}{2} \sum_{\substack{j,j' \\ j \neq j'}} N_j N_{j'} (u_{jj'jj'} \pm u_{jj'j'j}) + \frac{1}{2} \sum_j N_j (N_j - 1) u_{jjjj}. \quad (8.121)$$

The corollaries of this important result are very different for bosons and fermions. In the former case, the last term usually dominates, because the matrix elements (8.115) are typically the largest when all basis functions coincide. Note that this term allows a very simple interpretation: the number of the diagonal matrix elements it sums up for each state ( $j$ ) is just the number of interacting particle pairs residing in that state.

In contrast, for fermions the last term is zero, and the interaction energy is the difference of the two terms inside the first parentheses. In order to spell them out, let us consider the case when there is no direct spin–orbit interaction. Then the vectors

$|\beta\rangle_j$  of the single-particle state basis may be represented as direct products  $|o_j\rangle \otimes |m_j\rangle$  of their orbital and spin-orientation parts. (Here, for brevity, I am using  $m$  instead of  $m_s$ .) For spin- $1/2$  particles, including electrons, these orientations  $m_j$  may equal only either  $+1/2$  or  $-1/2$ ; in this case the spin part of the first matrix element,  $u_{jj'}$ , equals

$$\langle m | \otimes \langle m' | | m \rangle \otimes | m' \rangle, \quad (8.122)$$

where, as in the general Eq. (8.115), the position of a particular vector in a direct product codes the particle's number. Since the spins of different particles are defined in different Hilbert spaces, we may move their vectors around to get

$$\langle m | \otimes \langle m' | | m \rangle \otimes | m' \rangle = (\langle m | m \rangle)_1 \times (\langle m' | m' \rangle)_2 = 1, \quad (8.123)$$

for any pair of  $j$  and  $j'$ . On the other hand, the second matrix element,  $u_{jj'}$ , is proportional to

$$\langle m | \otimes \langle m' | | m' \rangle \otimes | m \rangle = (\langle m | m' \rangle)_1 \times (\langle m' | m \rangle)_2 = \delta_{mm'}. \quad (8.124)$$

In this case, it is convenient to rewrite Eq. (8.121) in the coordinate representation, using single-particle wavefunctions called *spin-orbitals*

$$\psi_j(\mathbf{r}) \equiv \langle \mathbf{r} | \beta_j \rangle = (\langle \mathbf{r} | o \rangle \otimes | m \rangle)_j. \quad (8.125)$$

They differ from the spatial parts of the usual orbital wavefunctions of the type (4.233) only in that their index  $j$  should be understood as the set of the orbital-state and the spin-orientation indices<sup>31</sup>. Also, due to the Pauli-principle restriction of numbers  $N_j$  to either 0 or 1, Eq. (8.121) may be also rewritten without the explicit occupancy numbers, with the understanding that the summation is extended only over the pairs of occupied states. As a result, it becomes

$$E_{\text{int}}^{(1)} = \frac{1}{2} \sum_{\substack{j,j' \\ j \neq j'}} \int d^3r \int d^3r' \begin{bmatrix} \psi_j^*(\mathbf{r}) \psi_{j'}^*(\mathbf{r}') u_{\text{int}}(\mathbf{r}, \mathbf{r}') \psi_j(\mathbf{r}) \psi_{j'}(\mathbf{r}') \\ - \psi_j^*(\mathbf{r}) \psi_{j'}^*(\mathbf{r}') u_{\text{int}}(\mathbf{r}, \mathbf{r}') \psi_{j'}(\mathbf{r}) \psi_j(\mathbf{r}') \end{bmatrix}. \quad (8.126)$$

In particular, for a system of two electrons, we may limit the summation to just two states ( $j, j' = 1, 2$ ). As a result, we return to Eqs. (8.39)–(8.41), with the bottom (minus) sign in Eq. (8.39), corresponding to the triplet spin states. Hence, Eq. (8.126) may be considered as the generalization of the direct and exchange interaction balance picture to an arbitrary number of orbitals and an arbitrary total number  $N$  of electrons. Note, however, that this equation cannot correctly describe the energy of the singlet spin state, corresponding to the plus sign in Eq. (8.39), and also of the

<sup>31</sup> The spin-orbitals (8.125) are also close to spinors (8.13), besides that the former definition takes into account that the spin  $s$  of a single particle is fixed, so that the spin-orbital may be indexed by the spin's orientation  $m \equiv m_s$  only. Also, if an orbital index is used, it should be clearly distinguished from  $j$ , i.e. the set of the orbital and spin indices. This is why I believe that the frequently met notation of spin-orbitals as  $\psi_{j,s}(\mathbf{r})$  may lead to confusion.

entangled triplet state<sup>32</sup>. The reason is that the description of entangled spin states, given in particular by Eqs. (8.18) and (8.20), requires *linear superpositions* of different Dirac states. (A proof of this fact is left for the reader’s exercise.)

Now comes a very important fact: the *approximate* result (8.126), added to the sum of unperturbed energies  $\epsilon_j^{(0)}$ , equals the sum of *exact* eigenenergies of the so-called *Hartree–Fock equation*<sup>33</sup>:

$$\left(-\frac{\hbar^2}{2m}\nabla^2 + u(\mathbf{r})\right)\psi_j(\mathbf{r}) + \sum_{j' \neq j} \int [\psi_{j'}^*(\mathbf{r}')u_{\text{int}}(\mathbf{r}, \mathbf{r}')\psi_j(\mathbf{r})\psi_{j'}(\mathbf{r}') - \psi_{j'}^*(\mathbf{r}')u_{\text{int}}(\mathbf{r}, \mathbf{r}')\psi_j(\mathbf{r})\psi_{j'}(\mathbf{r})]d^3r' = \epsilon_j\psi_j(\mathbf{r}), \quad (8.127)$$

where  $u(\mathbf{r})$  is the external-field potential acting on each particle separately—see the second of Eqs. (8.79). An advantage of this equation in comparison with Eq. (8.126) is that it allows the (approximate) calculation of not only the energy spectrum of the system, but also the corresponding spin–orbitals, taking into account their electron–electron interaction. Of course Eq. (8.127) is an *integro-differential* rather than just differential equation. There are, however, efficient methods of numerical solution of such equations, typically based on iterative methods. One more important trick is the exclusion of the filled internal electron shells (see section 3.7) from the explicit calculations, because the shell states are virtually unperturbed by the valence electron effects involved in typical atomic phenomena and chemical reactions. In this approach, the Coulomb field of the shells, described by fixed, pre-calculated and tabulated *pseudo-potentials*, is added to that of the nuclei. This approach dramatically cuts the computing resources necessary for systems of relatively heavy atoms, enabling a pretty accurate simulation of electronic and chemical properties of rather complex molecules, with thousands of electrons<sup>34</sup>. As a result, the Hartree–Fock approximation has become the de-facto baseline of all so-called *ab initio* (‘first-principle’) calculations in the most important field of quantum chemistry<sup>35</sup>.

In departures from this baseline, there are two opposite trends. For larger accuracy (and typically smaller systems), several ‘post-Hartree–Fock methods’, notably including the *configuration interaction method*<sup>36</sup>, that are more complex but may provide higher accuracy, have been developed.

<sup>32</sup> Indeed, due to the condition  $j' \neq j$ , and Eq. (8.124), the calculated negative exchange interaction is limited to electron state pairs with the same spin direction—such as the factorable triplet states ( $\uparrow\uparrow$  and  $\downarrow\downarrow$ ) of a two-electron system, in which the contribution of  $E_{\text{ex}}$ , given by Eq. (8.41), to the total energy is also negative.

<sup>33</sup> This equation was suggested in 1929 by D Hartree for the direct interaction, and extended to the exchange interaction by V Fock in 1930. In order to verify its equivalence to Eq. (8.126), it is sufficient to multiply all terms of Eq. (8.127) by  $\psi_j^*(\mathbf{r})$ , integrate them over all  $\mathbf{r}$  space (so that the right-hand side would give  $\epsilon_j$ ), and then sum these single-particle energies over all occupied states  $j$ .

<sup>34</sup> For condensed-matter systems, this and other computational methods are applied to single elementary spatial cells, with a limited number of electrons in them, using cyclic boundary conditions.

<sup>35</sup> See, e.g. [2].

<sup>36</sup> That method, in particular, allows the calculation of proper linear superpositions of the Dirac states (such as the entangled states for  $N = 2$ , discussed above) which are missing in the generic Hartree–Fock approach—see, e.g. the just-cited monograph by Szabo and Ostlund.



There is also a strong opposite trend of extending *ab initio* methods to larger systems, while sacrificing the results' accuracy and reliability. The ultimate case of this trend is applicable when the single-particle wavefunction overlaps are small and hence the exchange interaction is negligible, the last term in the square brackets of Eq. (8.127) may be ignored, the term  $\psi_j(\mathbf{r})$  may be taken out of the integral, and it is reduced to a differential equation, which is formally just the Schrödinger equation for a single particle in the following self-consistent effective potential:

$$u_{\text{ef}}(\mathbf{r}) = u(\mathbf{r}) + u_{\text{dir}}(\mathbf{r}), \quad u_{\text{dir}}(\mathbf{r}) = \sum_{j' \neq j} \int \psi_{j'}^*(\mathbf{r}') u_{\text{int}}(\mathbf{r}, \mathbf{r}') \psi_{j'}(\mathbf{r}') d^3r'. \quad (8.128)$$

This is the so-called *Hartree approximation*—that gives reasonable results for some systems<sup>37</sup>, especially those with low electron density. However, in dense electron systems (such as typical atoms, molecules, and condensed matter) the exchange interaction, described by the second term in the square brackets of Eqs. (8.126) and (8.127), may be as high as  $\sim 30\%$  of the direct interaction, and frequently cannot be ignored.

The tendency of taking this interaction in the simplest possible form is currently dominated by the *Density Functional Theory*<sup>38</sup>, universally known by its acronym DFT. In this approach, the equation solved for each eigenfunction  $\psi_j(\mathbf{r})$  is a differential, Schrödinger-like *Kohn–Sham equation*

$$\left[ -\frac{\hbar^2}{2m} \nabla^2 + u(\mathbf{r}) + u_{\text{dir}}^{\text{KS}}(\mathbf{r}) + u_{\text{xc}}(\mathbf{r}) \right] \psi_j(\mathbf{r}) = \varepsilon_j \psi_j(\mathbf{r}), \quad (8.129)$$

where

$$u_{\text{dir}}^{\text{KS}}(\mathbf{r}) = -e\phi(\mathbf{r}), \quad \phi(\mathbf{r}) = \frac{1}{4\pi\epsilon_0} \int d^3r' \frac{\rho(\mathbf{r}')}{|\mathbf{r} - \mathbf{r}'|}, \quad \rho(\mathbf{r}) = -en(\mathbf{r}), \quad (8.130)$$

and  $n(\mathbf{r})$  is the total electron density in a particular point, calculated as

$$n(\mathbf{r}) \equiv \sum_j \psi_j^*(\mathbf{r}) \psi_j(\mathbf{r}). \quad (8.131)$$

The most important feature of the Kohn–Sham Hamiltonian is the simplified description of the exchange and correlation effects by the effective *exchange–correlation* potential  $u_{\text{xc}}(\mathbf{r})$ . This potential is calculated in various approximations, most valid only in the limit when the number of electrons in the system is very high. The simplest of them (proposed by Kohn *et al* in the 1960s) is the *Local Density Approximation* (LDA) in which the effective exchange potential at each point is a

<sup>37</sup> An extreme example the Hartree approximation is the *Thomas–Fermi model* of heavy atoms (with  $Z \gg 1$ ), in which atomic electrons, at each distance  $r$  from the nucleus, are treated as an ideal, uniform Fermi gas, with a certain density  $n(r)$  corresponding to the local value  $u_{\text{ef}}(r)$ , but a common value of their highest full single-particle energy,  $\varepsilon = 0$ , to ensure the equilibrium. (The analysis of this model is left for the reader's exercise.)

<sup>38</sup> It had been developed by W Kohn and his associates in 1965–66, and eventually (in 1998) was marked with a Nobel Prize in Chemistry.

function only of the electron density (8.131) at the same point, taken from the theory of a *uniform* gas of free electrons<sup>39</sup>. However, for many tasks of quantum chemistry, the accuracy given by the LDA is insufficient, because inside molecules the density  $n$  typically changes very fast. As a result, the DFT has become widely accepted in this field only after the introduction, in the 1980s, of more accurate, though more cumbersome models for  $u_{xc}(\mathbf{r})$ , notably the so-called *Generalized Gradient Approximations* (GGAs).

Due to its relative simplicity, the DFT enables the calculation, with the same computing resources and reasonable precision, some properties of much larger systems than the methods based on the Hartree–Fock theory. As a result, it has become a very popular tool of *ab initio* calculations<sup>40</sup>. Please note, however, that despite this undisputable success, this approach has its problems. From my personal point of view, the most offensive of them is the implicit assumption of the unphysical Coulomb interaction of an electron with itself (by dropping, on the way from Eq. (8.128) to Eq. (8.130), the condition  $j' \neq j$  at the calculation of  $u_{dir}^{KS}$ ). As a result of these issues, for a reasonable description of some effects, the available DFT packages are either inapplicable at all or require substantial artificial tinkering<sup>41</sup>. Unfortunately, because of lack of time, for details I have to refer the reader to specialized literature<sup>42</sup>.

## 8.5 Quantum computation and cryptography

Now I have to review the emerging fields of *quantum computation* and *encryption*<sup>43</sup>. These fields are currently the subject of a very intensive research effort, which has already brought (besides much hype) some results of general importance. My coverage, by necessity short, will focus on these results, referring the reader interested in details to special literature<sup>44</sup>. Because of the very active stage of the fields, I will also provide, in the last part of the section, quite a few references to recent publications, making its style closer to a brief research review than to a part of a textbook.

Presently, most work on quantum computation and encryption is based on systems of spatially-separated (and hence *distinguishable*) two-level systems—in this context, commonly called *qubits*<sup>45</sup>. Due to this distinguishability, the issues that were

<sup>39</sup> Just for the reader's reference: for a uniform, degenerate Fermi-gas of electrons (with the Fermi energy  $\epsilon_F \gg k_B T$ ), the most important, exchange part  $u_x$  of  $u_{xc}$  may be calculated analytically:  $u_x = -(3/4\pi)e^2 k_F / 4\pi\epsilon_0$ , where the Fermi momentum  $k_F = (2m_e \epsilon_F)^{1/2} / \hbar$  is defined by the electron density:  $n = 2(4\pi/3)k_F^3 / (2\pi)^3 \equiv k_F^3 / 3\pi^2$ .

<sup>40</sup> This popularity is enhanced by the availability of several advanced DFT software packages, some of them (such as SIESTA, see <https://departments.icmab.es/leem/siesta/>) in public domain.

<sup>41</sup> As just a few examples, see [3–5].

<sup>42</sup> See, e.g. either the monograph by [6], or the later textbook [7]. For a popular recent review, and references to more recent work in this still-developing field, see [8].

<sup>43</sup> Since these fields are much related, they are often referred to under the common title of 'quantum information science', though this term is somewhat misleading, obscuring the physical aspects of the field.

<sup>44</sup> Despite the recent flood of new books on the field, one of its first surveys, [9], is perhaps still the best one.

<sup>45</sup> In some texts, the term qubit (or 'Qbit', or 'Q-bit') is used instead for the *information contents* of a two-level system—very much like the classical bit of information (in this context, frequently called 'Cbit' or 'C-bit') describes the information contents of a classical bistable system—see, e.g. *Part SM* section 2.2.

the focus of the first sections of this chapter, including the second quantization approach, are irrelevant here. On the other hand, systems of qubits have some interesting properties that have not been discussed in this course yet.

First of all, a system of  $N \gg 1$  qubits may contain much more information than the same number of  $N$  classical bits. Indeed, according to the discussions in chapter 4 and section 5.1, an arbitrary pure state of a single qubit may be represented by its ket vector (4.37)—see also Eq. (5.1):

$$|\alpha\rangle_{N=1} = \alpha_1|u_1\rangle + \alpha_2|u_2\rangle, \quad (8.132)$$

where  $\{u_j\}$  is any orthonormal two-state basis. It is natural and common to employ, as  $u_j$ , the eigenstates  $a_j$  of the observable  $A$  that is eventually measured in the particular physical implementation of the qubit—say, a certain Cartesian component of spin- $1/2$ . It is also common to write the kets of these base states as  $|0\rangle$  and  $|1\rangle$ ,<sup>46</sup> so that Eq. (8.132) takes the form

$$|\alpha\rangle_{N=1} = a_0|0\rangle + a_1|1\rangle \equiv \sum_{j=0,1} a_j|j\rangle. \quad (8.133)$$

(Here, and in the balance of this section, the letter  $j$  is used to denote an integer equal to either 0 or 1.) According to this relation, any state  $\alpha$  of a qubit is completely defined by two complex  $c$ -numbers  $a_j$ , i.e. by four real numbers. Moreover, due to the normalization condition  $|a_1|^2 + |a_2|^2 = 1$ , we need just three independent real numbers—say, the Bloch sphere coordinates  $\theta$  and  $\varphi$  (see figure 5.3), plus the common phase  $\gamma$ , which becomes important only when we consider coherent states of a several-qubit system.

This is a good time to note that a qubit is very different from any classical bistable system used to store single bits of information—such as two possible voltage states of the usual SRAM cell (a positive-feedback loop of two transistor-based inverters). Namely, the stationary states of a classical bistable system, due to its nonlinearity, are stable with respect to small perturbations, so that they may be rather robust with respect to unintentional interaction with its environment. In contrast, the qubit's state may be readily disturbed (i.e. its representation point on the Bloch sphere shifted) by even minor perturbations, because it does not have such internal state stabilization mechanism<sup>47</sup>. Due to this reason, qubit-based systems are rather vulnerable to environment-induced drifts, including the dephasing and relaxation discussed in the previous chapter, creating major experimental challenges—see below.

Now, if we have a system of 2 qubits, the vector (4.37) of its arbitrary pure state may be represented as a sum of  $2^2 = 4$  terms<sup>48</sup>,

<sup>46</sup> In this notation, at the Bloch sphere representation (figure 5.3), the North Pole state (that is traditionally denoted as  $\uparrow$  in quantum mechanics) is taken for 0, and the South Pole state  $\downarrow$  for 1, so that in Eq. (8.133),  $a_0 = \cos(\theta/2)$ ,  $a_1 = \sin(\theta/2)\exp\{i\varphi\}$ .

<sup>47</sup> In this aspect as well, the information processing systems based on qubits are closer to classical analog computers (which were popular once, but are now virtually abandoned) rather than classical digital ones.

<sup>48</sup> Here and in most instances below I use the same shorthand notation as was used in the beginning of this chapter—cf. Eq. (8.1). In this short form, qubit's number is coded by the order of its state index inside the single ket-vector, while in the long form, such as in Eq. (8.137), it is coded by the order of single-qubit vectors.

$$|\alpha\rangle_{N=2} = a_{00}|00\rangle + a_{01}|01\rangle + a_{10}|10\rangle + a_{11}|11\rangle \equiv \sum_{j_1, j_2=0,1} a_{j_1 j_2} |j_1 j_2\rangle, \quad (8.134)$$

with four complex coefficients, i.e.  $4 \times 2 = 8$  real numbers, subject to just one normalization condition, which follows from the requirement  $\langle\alpha|\alpha\rangle = 1$ :

$$\sum_{j_1, j_2=0,1} |a_{j_1 j_2}|^2 = 1. \quad (8.135)$$

The evident generalization of Eqs. (8.133) and (8.134) to an arbitrary pure state of an  $N$ -qubit system is given by a sum of  $2^N$  terms:

$$|\alpha\rangle_N = \sum_{j_1, j_2, \dots, j_N=0,1} a_{j_1 j_2 \dots j_N} |j_1 j_2 \dots j_N\rangle, \quad (8.136)$$

including all possible combinations of 0s and 1s inside the ket, so that the state is fully described by  $2^N$  complex numbers, i.e.  $2 \cdot 2^N = 2^{N+1}$  real numbers, with only one constraint, similar to Eq. (8.135), imposed by the normalization condition. Let me emphasize that this exponential growth of the information contents would not be possible without the qubit state entanglement. Indeed, in the particular case when qubit states are unentangled (factorable),

$$|\alpha\rangle_N = |\alpha_1\rangle|\alpha_2\rangle \dots |\alpha_N\rangle, \quad (8.137)$$

where each  $|\alpha_n\rangle$  is described by an equality similar to Eq. (8.133) with its individual expansion coefficients, the system state description requires only  $3N - 1$  real numbers—e.g.  $N$  sets  $\{\theta, \varphi, \gamma\}$  less one common phase.

However, it would be wrong to project this exponential growth of information contents directly on the capabilities of quantum computation, because this process has to include the output information readout, i.e. qubit state measurements. Due to the fundamental intrinsic uncertainty of quantum systems, the measurement of a single qubit even in a pure state (8.133) generally may give either of two results, with probabilities  $W_0 = |a_0|^2$  and  $W_1 = |a_1|^2$ . In order to comply with the general notion of computation, any quantum computer has to provide certain (or virtually certain) results, and hence the probabilities  $W_j$  have to be very close to either 0 or 1, so that before the measurement, each measured qubit has to be in a basis state—either 0 or 1. This means that the computational system with  $N$  output qubits, just before the final readout, has to be in one of the factorable states

$$|\alpha\rangle_N = |j_1\rangle|j_2\rangle \dots |j_N\rangle \equiv |j_1 j_2 \dots j_N\rangle, \quad (8.138)$$

which is a very small subset even of the set of all unentangled states (8.137), and whose maximum information contents is just  $N$  classical bits.

Now the reader may start thinking that this constraint strips quantum computations of any advantages over their classical counterparts, but this view is also

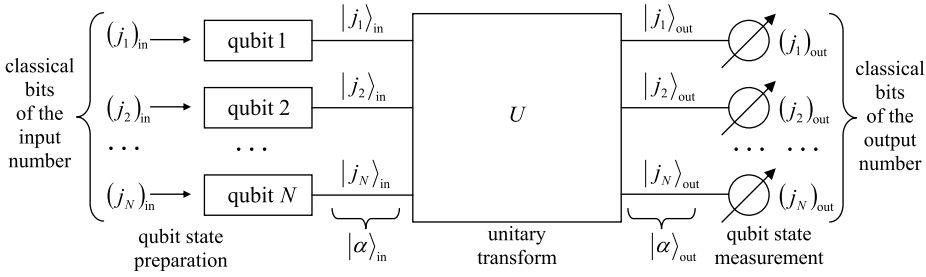


Figure 8.3. The baseline scheme of quantum computation.

superficial. In order to show that, let us consider the scheme of the most actively explored type of quantum computation, shown in figure 8.3.<sup>49</sup>

Here each horizontal line (sometimes called a ‘wire’<sup>50</sup>) corresponds to a single qubit, tracing its time evolution in the same direction as at the usual time function plots: from left to right. This means that the left column  $|\alpha\rangle_{\text{in}}$  of ket-vectors describes the initial state of the qubits<sup>51</sup>, while the right column  $|\alpha\rangle_{\text{out}}$  describes their final (pre-measurement) state. The box labeled  $U$  represents the qubit evolution in time due to their specially arranged interactions between each other and/or external drive ‘forces’. Besides these forces, during this evolution the system is supposed to be ideally isolated from the dephasing and energy-dissipating environment, so that the evolution may be described by a unitary operator defined in the  $2^N$ -dimensional Hilbert space of  $N$  qubits:

$$|\alpha\rangle_{\text{out}} = \hat{U}|\alpha\rangle_{\text{in}}. \quad (8.139)$$

With the condition that the input and output states have the simple form (8.138), this equality reads

$$|(j_1)_{\text{out}}(j_2)_{\text{out}}\dots(j_N)_{\text{out}}\rangle = \hat{U}|(j_1)_{\text{in}}(j_2)_{\text{in}}\dots(j_N)_{\text{in}}\rangle. \quad (8.140)$$

<sup>49</sup> Numerous modifications of this ‘baseline’ scheme have been suggested, for example with the number of output qubits different from that of input qubits, etc. Some other options are discussed at the end of this section.

<sup>50</sup> The notion of ‘wires’ stems from the similarity between these diagrams and the drawings used to describe classical computation circuits (see, e.g. figure 8.4a below); in the classical case the lines may be indeed understood as physical wires connecting physical devices: logic gates and/or memory cells. In this context, note that classical computer components also have nonvanishing time delays, so that even in this case the left-to-right device ordering is useful to indicate the timing of (and frequently the causal relation between) the signals.

<sup>51</sup> As follows from our discussions in chapter 7, the preparation of a pure state (8.133) is (conceptually) straightforward. Placing a qubit into a weak contact with an environment of temperature  $T \ll \Delta/k_B$ , where  $\Delta$  is the difference between energies of the eigenstates 0 and 1, we may achieve its relaxation into the lowest-energy state. Then, if the qubit must be set into a different pure state, it may be driven there by the application of a pulse of a proper external classical ‘force’. For example, if an actual spin- $\frac{1}{2}$  is used as qubits, a pulse of magnetic field with proper direction and duration may be applied to arrange its torque-induced precession to the required Bloch sphere point—see figure 5.3c. In most qubit systems, using a proper part of the Rabi oscillation period (see section 6.5) is more practicable for this purpose.

The art of quantum computer design consists of selecting such unitary operators  $\hat{U}$  that would:

- satisfy Eq. (8.140),
- be physically implementable, and
- enable substantial performance advantages of the quantum computation over its classical counterparts with similar functionality, at least for some digital functions (algorithms).

I will have time/space to demonstrate the possibility of such advantages on just one, perhaps the simplest example—the so-called *Deutsch problem*<sup>52</sup>. Let us consider the family of single-bit classical Boolean functions  $j_{\text{out}} = f(j_{\text{in}})$ . Since both  $j$  are Boolean variables, i.e. may take only values 0 and 1, there are evidently only four such functions<sup>53</sup>:

$f$	$f(0)$	$f(1)$	class	$F$	$f(1)-f(0)$
$f_1$	0	0	constant	0	0
$f_2$	0	1	balanced	1	1
$f_3$	1	0	balanced	1	-1
$f_4$	1	1	constant	0	0

(8.141)

Of them, the functions  $f_1$  and  $f_4$ , whose values are independent of their arguments, are called *constants*, while the functions  $f_2$  (called ‘YES’ or ‘IDENTITY’) and  $f_3$  (‘NOT’ or ‘INVERSION’) are called *balanced*. The Deutsch problem is to determine the class of a single-bit function, implemented with a ‘black box’, as being either constant or balanced, using just one experiment.

Classically, this is clearly impossible, and the simplest way to perform the function’s classification involves two similar black boxes  $f$ —see figure 8.4a.<sup>54</sup> This solution uses the so-called *exclusive-OR* (for short, XOR) *gate* whose output is described by the following function  $F$  of its two Boolean arguments  $j_1$  and  $j_2$ :<sup>55</sup>

$$F(j_1, j_2) = j_1 \oplus j_2 \equiv \begin{cases} 0, & \text{if } j_1 = j_2, \\ 1, & \text{if } j_1 \neq j_2. \end{cases} \quad (8.142)$$

In the particular circuit shown in figure 8.4a, the gate produces the following output:

$$F = f(0) \oplus f(1), \quad (8.143)$$

<sup>52</sup>It is named after D Deutsch, whose 1985 paper (motivated by an inspirational but not very specific publication by R Feynman in 1982) launched the whole field of quantum computation.

<sup>53</sup>The function  $F$  will be defined imminently—see Eq. (8.142).

<sup>54</sup>Alternatively, we may perform two sequential experiments on the same black box  $f$ , first recording and then recalling the first experiment’s result. However, the Deutsch problem calls for a single experiment.

<sup>55</sup>The XOR sign  $\oplus$  should not be confused with the sign  $\otimes$  of the direct product of state vectors (which in this section is just implied).

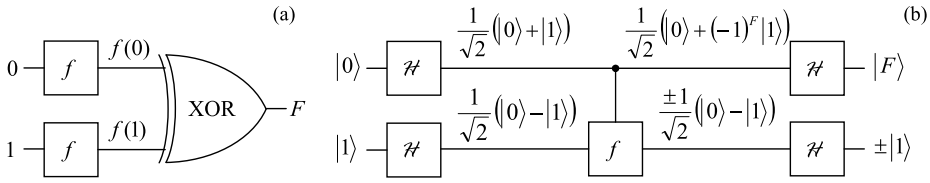


**Figure 8.4.** The simplest (a) classical and (b) quantum ways to classify a single-bit Boolean function  $f$ .

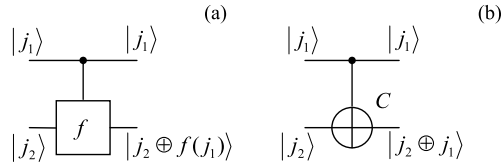


**Figure 8.5.** Two-qubit quantum gates: (a) a two-qubit function  $f$  and (b) its particular case  $C$  (CNOT), and their actions on a basis state.

which is equal to 1 if  $f(0) \neq f(1)$ , i.e. if the function  $f$  is balanced, and to 0 in the opposite case—see the 5th column in Eq. (8.141).

On the other hand, as will be proved below, all four functions  $f$  may be implemented quantum-mechanically, for example as a unitary transform of two input qubits, acting as follows on each basis component  $|j_1 j_2\rangle \equiv |j_1\rangle|j_2\rangle$  of the general input state (8.134):

$$\hat{f} |j_1\rangle|j_2\rangle = |j_1\rangle|j_2 \oplus f(j_1)\rangle, \quad (8.144)$$

where  $f$  is any of the classical Boolean functions listed in the table of Eq. (8.141)—see figure 8.5a.

In the particular case when  $f$  in Eq. (8.144) is just the YES function:  $f(j) = f_2(j) = j$ , this ‘circuit’ is reduced to the so-called *CNOT gate*, a key ingredient of many other quantum computation schemes, performing the following two-qubit transform:

$$\hat{C} |j_1 j_2\rangle = |j_1\rangle|j_2 \oplus j_1\rangle. \quad (8.145a)$$

Let us use Eq. (8.142) to spell out this function for all four possible input qubit combinations:

$$\hat{C}|00\rangle = |00\rangle, \quad \hat{C}|01\rangle = |01\rangle, \quad \hat{C}|10\rangle = |11\rangle, \quad \hat{C}|11\rangle = |10\rangle. \quad (8.145b)$$

In plain English, this means that acting on a basis state  $j_1 j_2$ , the CNOT gate leaves the state of the first, *source* qubit (shown by the upper lines in figure 8.5) intact, but flips the state of the second, *target* qubit if the first one is in the basis state 1. In even simpler words, the state  $j_1$  of the source qubit controls the NOT function acting on the target qubit—hence the gate’s name CNOT (the semi-acronym of ‘Controlled NOT’).

For the quantum function (8.144), with an arbitrary and unknown  $f$ , the Deutsch problem may be solved within the general scheme shown in figure 8.3, with the particular structure of the unitary-transform box  $U$  spelled out in figure 8.4b, which involves just one implementation of the function  $f$ . Here the single-qubit quantum gate  $\hat{H}$  performs the so-called *Hadamard* (or ‘Walsh–Hadamard’) transform<sup>56</sup>, whose operator is defined by the following actions on the qubit’s basis states:

$$\hat{H}|0\rangle = \frac{1}{\sqrt{2}}(|0\rangle + |1\rangle), \quad \hat{H}|1\rangle = \frac{1}{\sqrt{2}}(|0\rangle - |1\rangle), \quad (8.146)$$

—see also the two leftmost state label columns in figure 8.4b.<sup>57</sup> Since its quantum-mechanical operator has to be linear (to be physically realistic), it needs to perform the action (8.146) on the basis states even when they are parts of an arbitrary linear superposition—as they are, for example, for the two right Hadamard gates in figure 8.4b. For example, as immediately follows from Eqs. (8.146) and the operator’s linearity,

$$\begin{aligned} \hat{H}(\hat{H}|0\rangle) &= \hat{H}\left(\frac{1}{\sqrt{2}}(|0\rangle + |1\rangle)\right) = \frac{1}{\sqrt{2}}\hat{H}(|0\rangle + |1\rangle) \\ &= \frac{1}{\sqrt{2}}\left(\frac{1}{\sqrt{2}}(|0\rangle + |1\rangle) + \frac{1}{\sqrt{2}}(|0\rangle - |1\rangle)\right) = |0\rangle, \end{aligned} \quad (8.147a)$$

Absolutely similarly, we may get<sup>58</sup>

$$\hat{H}(\hat{H}|1\rangle) = |1\rangle. \quad (8.147b)$$

Now let us carry out a sequential analysis of the ‘circuit’ shown in figure 8.4b. Since the input states of the gate  $f$  in this particular circuit are described by Eqs. (8.146), its output state’s ket is

$$\begin{aligned} \hat{f}(\hat{H}|0\rangle\hat{H}|1\rangle) &= \hat{f}\left(\frac{1}{\sqrt{2}}(|0\rangle + |1\rangle)\frac{1}{\sqrt{2}}(|0\rangle - |1\rangle)\right) \\ &= \frac{1}{2}(\hat{f}|00\rangle - \hat{f}|01\rangle + \hat{f}|10\rangle - \hat{f}|11\rangle). \end{aligned} \quad (8.148)$$

Now we may apply Eq. (8.144) to each basis ket to get:

<sup>56</sup>In order to exclude any chance of confusion between the Hadamard transform’s operator  $\hat{H}$  and the Hamiltonian operator  $\hat{H}$ , they are typeset using different fonts.

<sup>57</sup>Note that according to Eq. (8.146), the operator  $\hat{H}$  does *not* belong to the class  $\hat{U}$  described by Eq. (8.140)—while the whole ‘circuit’ shown in figure 8.4b, does—see below.

<sup>58</sup>Since the states 0 and 1 form a full basis of a single qubit, both Eqs. (8.147) may be summarized as an operator equality:  $\hat{H}^2 = \hat{I}$ . It is also easy to check that the Hadamard transform of an arbitrary state may be represented on the Bloch sphere (figure 5.3) as a  $\pi$ -rotation about the axis that bisects the angle between  $x$  and  $z$ .



$$\begin{aligned}
 & \hat{f} |00\rangle - \hat{f} |01\rangle + \hat{f} |10\rangle - \hat{f} |11\rangle \\
 & \equiv \hat{f} |0\rangle|0\rangle - \hat{f} |0\rangle|1\rangle + \hat{f} |1\rangle|0\rangle - \hat{f} |1\rangle|1\rangle \\
 & = |0\rangle|0 \oplus f(0)\rangle - |0\rangle|1 \oplus f(0)\rangle + |1\rangle|0 \oplus f(1)\rangle - |1\rangle|1 \oplus f(1)\rangle \\
 & \equiv |0\rangle(|0 \oplus f(0)\rangle - |1 \oplus f(0)\rangle) + |1\rangle(|0 \oplus f(1)\rangle - |1 \oplus f(1)\rangle).
 \end{aligned} \tag{8.149}$$

Note that the expression in the first parentheses, characterizing the state of the target qubit, is equal to  $(|0\rangle - |1\rangle) \equiv (-1)^0 (|0\rangle - |1\rangle)$  if  $f(0) = 0$  (and hence  $0 \oplus f(0) = 0$  and  $1 \oplus f(0) = 1$ ), and to  $(|1\rangle - |0\rangle) \equiv (-1)^1 (|0\rangle - |1\rangle)$  in the opposite case  $f(0) = 1$ , so that both cases may be described in one shot by rewriting the parentheses as  $(-1)^{f(0)} (|0\rangle - |1\rangle)$ . The second parentheses is absolutely similarly controlled by the value of  $f(1)$ , so that the outputs of the gate  $f$  are unentangled:

$$\begin{aligned}
 \hat{f}(\hat{\mathcal{R}}|0\rangle\hat{\mathcal{R}}|1\rangle) &= \frac{1}{2}((-1)^{f(0)}|0\rangle + (-1)^{f(1)}|1\rangle)(|0\rangle - |1\rangle) \\
 &= \pm \frac{1}{\sqrt{2}}(|0\rangle + (-1)^F|1\rangle) \frac{1}{\sqrt{2}}(|0\rangle - |1\rangle),
 \end{aligned} \tag{8.150}$$

where the last step has used the fact that the classical Boolean function  $F$ , defined by Eq. (8.142), equals  $\pm[f(1) - f(0)]$ —please compare the last two columns in Eq. (8.141). The front sign  $\pm$  in Eq. (8.150) may be prescribed to any of the component ket-vectors—for example to that of the target qubit, as shown by the third column of state labels in figure 8.4b.

This intermediate result is already rather remarkable. Indeed, it shows that, despite the impression one could get from figure 8.5, the gates  $f$  and  $C$ , being ‘controlled’ by the source qubit, may change that qubit’s state as well! This fact (partly reflected by the vertical direction of the control lines in figures 8.4 and 8.5, symbolizing the same stage of system’s time evolution) shows how careful one should be interpreting quantum-computational ‘circuits’, thriving on qubits’ entanglement, because the ‘signals’ on different sections of a ‘wire’ may differ—see figure 8.4b again.

At the last stage of the circuit shown in figure 8.4b, the qubit components of the state (8.150) are fed into one more pair of Hadamard gates, whose outputs therefore are

$$\begin{aligned}
 \hat{\mathcal{R}}\left(\frac{1}{\sqrt{2}}(|0\rangle + (-1)^F|1\rangle)\right) &= \frac{1}{\sqrt{2}}(\hat{\mathcal{R}}|0\rangle + (-1)^F\hat{\mathcal{R}}|1\rangle), \quad \text{and} \\
 \hat{\mathcal{R}}\left(\pm\frac{1}{\sqrt{2}}(|0\rangle - |1\rangle)\right) &= \pm\frac{1}{\sqrt{2}}(\hat{\mathcal{R}}|1\rangle - \hat{\mathcal{R}}|0\rangle).
 \end{aligned} \tag{8.151}$$

Now using Eqs. (8.146) again, we see that the output state ket-vectors of the source and target qubits are, respectively,

$$\frac{1 + (-1)^F}{2}|0\rangle + \frac{1 - (-1)^F}{2}|1\rangle, \quad \text{and} \quad \pm|1\rangle. \tag{8.152}$$

Since, according to Eq. (8.142), the Boolean function  $F$  may take only values 0 or 1, the final state of the source qubit is always one of its basis states  $j$ , namely the one with  $j = F$ . Its measurement tells us whether the function  $f$ , participating in Eq. (8.144), is constant or balanced—see Eq. (8.141) again<sup>59</sup>.

Thus, the quantum circuit shown in figure 8.4b indeed solves the Deutsch problem in one shot. Reviewing our analysis, we may see that this is possible because the unitary transform performed by the quantum gate  $f$  is applied to the entangled states (8.146) rather than to the basis states. Due to this trick, the quantum state components depending on  $f(0)$  and  $f(1)$  are processed simultaneously, in parallel. This *quantum parallelism* may be extended to circuits with many ( $N \gg 1$ ) qubits and, for some tasks, provide a dramatic performance increase—for example, reducing the necessary circuit component number from  $O(2^N)$  to  $O(N^p)$ , where  $p$  is a finite (and not very big) number.

However, this efficiency comes at a high price. Indeed, let us discuss the possible physical implementation of quantum gates, starting from the Hadamard gate, which performs a single-qubit transform—see Eq. (8.146). With the linearity requirement, its action on the arbitrary state (8.133) should be

$$\begin{aligned} \hat{H}|\alpha\rangle &= a_0\hat{H}|0\rangle + a_1\hat{H}|1\rangle = a_0\frac{1}{\sqrt{2}}(|0\rangle + |1\rangle) + a_1\frac{1}{\sqrt{2}}(|0\rangle - |1\rangle) \\ &= \frac{1}{\sqrt{2}}(a_0 + a_1)|0\rangle + \frac{1}{\sqrt{2}}(a_0 - a_1)|1\rangle, \end{aligned} \quad (8.153)$$

meaning that the state probability amplitudes in the end ( $t = \mathcal{T}$ ) and beginning ( $t = 0$ ) of the qubit evolution in time have to be related as

$$a_0(\mathcal{T}) = \frac{a_0(0) + a_1(0)}{\sqrt{2}}, \quad a_1(\mathcal{T}) = \frac{a_0(0) - a_1(0)}{\sqrt{2}}. \quad (8.154)$$

This task may be again performed using the Rabi oscillations, which were discussed in section 6.5, i.e. by applying to the qubit (a two-level system), for a limited time period  $\mathcal{T}$ , a weak sinusoidal external signal of frequency  $\omega$  equal to the intrinsic quantum oscillation frequency  $\omega_{nn'}$  defined by Eq. (6.85). A perturbative analysis of the Rabi oscillations was carried out in section 6.5, even for nonvanishing (though small) detuning  $\Delta = \omega - \omega_{nn'}$ , but only for the particular initial conditions when at  $t = 0$  the system was in one on the basis states (there labeled as  $n'$ ), i.e. another state (there labeled  $n$ ) was empty. For our current purposes we need to find the amplitudes  $a_{0,1}(t)$  for arbitrary initial conditions  $a_{0,1}(0)$ , subject only to the time-independent normalization condition  $|a_0|^2 + |a_1|^2 = 1$ . For the case of exact tuning,

<sup>59</sup>Note that the last Hadamard transform of the target qubit (i.e. the Hadamard gate shown in the lower right corner of figure 8.4b) is not necessary for the Deutsch problem's solution—though it should be included if we want the whole circuit to satisfy the general condition (8.140).

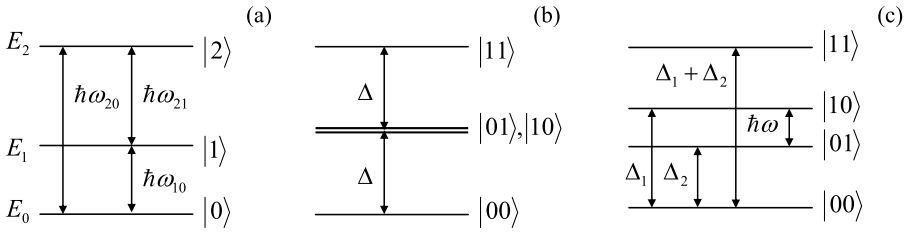


**Figure 8.6.** Energy-level schemes used for unitary transformations of (a) single qubits and (b, c) two-qubit systems.

$\Delta = 0$ , the solution of the system (6.94) is elementary<sup>60</sup>, and gives the following solution<sup>61</sup>:

$$\begin{aligned} a_0(t) &= a_0(0)\cos \Omega t - ia_1(0)e^{i\varphi} \sin \Omega t, \\ a_1(t) &= a_1(0)\cos \Omega t - ia_0(0)e^{-i\varphi} \sin \Omega t, \end{aligned} \quad (8.155)$$

where  $\Omega$  is the Rabi oscillation frequency (6.99), in the exact-tuning case proportional to the amplitude  $|A|$  of the external ac drive  $A = |A|\exp\{i\varphi\}$ —see Eq. (6.86). Comparing these expressions with Eqs. (8.154), we see that for  $t = \mathcal{T} = \pi/4\Omega$  and  $\varphi = \pi/2$  they ‘almost’ coincide, besides the opposite sign of  $a_1(\mathcal{T})$ . Conceptually the simplest way to correct this deficiency is to follow the *ac* ‘ $\pi/4$ -pulse’, just discussed, by a short *dc* ‘ $\pi$ -pulse’ of the duration  $\mathcal{T} = \pi/\delta$ , which temporarily creates a small additional energy difference  $\delta$  between the basis states 0 and 1. According to the basic Eq. (1.62), such a difference creates an additional phase difference  $\mathcal{T} = \delta/\hbar$  between the states, equal to  $\pi$  for the ‘ $\pi$ -pulse’.

Another way (that may be also useful for two-qubit operations) is to use another, auxiliary energy level  $E_2$  whose distances from the basic levels  $E_1$  and  $E_0$  are significantly different from the difference  $(E_1 - E_0)$ —see figure 8.6a. In this case, the weak external ac field tuned to any of three potential quantum transition frequencies  $\omega_{mn} \equiv (E_n - E_m)/\hbar$  initiates such transitions between the corresponding states only, with a negligible perturbation of the third state. (Such transitions may be again described by Eqs. (8.155), with the appropriate index changes.) For the Hadamard transform implementation, it is sufficient to apply (after the already discussed  $\pi/4$ -pulse of frequency  $\omega_{10}$ , and with the initially empty level  $E_2$ ), an additional  $\pi$ -pulse of frequency  $\omega_{20}$ , with any phase  $\varphi$ . Indeed, according to the first of Eqs. (8.155), with the due replacement  $a_1(0) \rightarrow a_2(0) = 0$ , such a pulse flips the sign of the amplitude  $a_0(t)$ , while the amplitude  $a_1(t)$ , not involved in this additional transition, remains unchanged.

Now let me describe the conceptually simplest (though, for some qubit types, not the most practically convenient) scheme for the implementation of the CNOT gate, whose action is described by a linear unitary operator satisfying Eq. (8.145). For

<sup>60</sup> An alternative way to analyze the qubit evolution is to use the Bloch equation (5.21), with an appropriate function  $\Omega(t)$  describing the control field.

<sup>61</sup> To comply with our current notation, the coefficients  $a_n'$  and  $a_n$  of section 6.5 are replaced with  $a_0$  and  $a_1$ .

that, evidently, the involved qubits have to interact for some time  $\mathcal{T}$ . As was repeatedly discussed in the two last chapters, in most cases such interaction of two subsystems is factorable—see Eq. (6.145). For qubits, i.e. two-level systems, each of the component operators may be represented by a  $2 \times 2$  matrix in the basis of the states 0 and 1. According to Eq. (4.106), such a matrix may be always expressed as a linear combination  $(bI + \mathbf{c} \cdot \boldsymbol{\sigma})$ , where  $b$  and three Cartesian components of the vector  $\mathbf{c}$  are  $c$ -numbers. Let us consider the simplest form of such factorable interaction Hamiltonian:

$$\hat{H}_{\text{int}}(t) = \begin{cases} \kappa \hat{\sigma}_z^{(1)} \hat{\sigma}_z^{(2)}, & \text{for } 0 < t < \mathcal{T}, \\ 0, & \text{otherwise,} \end{cases} \quad (8.156)$$

where the upper index is the qubit number, and  $\kappa$  is a  $c$ -number constant<sup>62</sup> According to Eq. (4.175), by the end of the interaction period, this Hamiltonian produces the following unitary transform:

$$\hat{U}_{\text{int}} = \exp \left\{ -\frac{i}{\hbar} \hat{H}_{\text{int}} \mathcal{T} \right\} \equiv \exp \left\{ -\frac{i}{\hbar} \kappa \hat{\sigma}_z^{(1)} \hat{\sigma}_z^{(2)} \mathcal{T} \right\}. \quad (8.157)$$

Since in the basis of unperturbed two-bit basis states  $|j_1 j_2\rangle$ , the product operator  $\hat{\sigma}_z^{(1)} \hat{\sigma}_z^{(2)}$  is diagonal, so is the unitary operator (8.157), with the following action on these states:

$$\hat{U}_{\text{int}} |j_1 j_2\rangle = \exp \{ i\theta \sigma_z^{(1)} \sigma_z^{(2)} \} |j_1 j_2\rangle, \quad (8.158)$$

where  $\theta = -\kappa \mathcal{T} / \hbar$ , and  $\sigma_z$  are the eigenvalues of the Pauli matrix  $\sigma_z$  for the basis states of the corresponding qubit:  $\sigma_z = +1$  for  $|j\rangle = |0\rangle$ , and  $\sigma_z = -1$  for  $|j\rangle = |1\rangle$ . Let me, for clarity, spell out Eq. (8.158) for the particular case  $\theta = -\pi/4$  (corresponding to the qubit coupling time  $\mathcal{T} = \pi \hbar / 4\kappa$ ):

$$\begin{aligned} \hat{U}_{\text{int}} |00\rangle &= e^{-i\pi/4} |00\rangle, & \hat{U}_{\text{int}} |01\rangle &= e^{i\pi/4} |01\rangle, \\ \hat{U}_{\text{int}} |10\rangle &= e^{i\pi/4} |10\rangle, & \hat{U}_{\text{int}} |11\rangle &= e^{-i\pi/4} |11\rangle. \end{aligned} \quad (8.159)$$

In order to compensate the undesirable parts of this joint phase shift of the basis states, let us now apply similar individual ‘rotations’ of each qubit by angle  $\theta' = +\pi/4$ ,

<sup>62</sup>The assumption of simultaneous time independence of the basis state vectors and the interaction operator (within the time interval  $0 < t < \mathcal{T}$ ) is possible only if the basis state energy difference  $\Delta$  of both qubits is exactly the same. For this case, the simple physical explanation of the time evolution (8.156) follows from figure 8.6b, c, which shows the spectrum of the total energy  $E = E_1 + E_2$  of the two-bit system. In the absence of interaction (figure 8.6b), the energies of two basis states,  $|01\rangle$  and  $|10\rangle$ , are equal, enabling even a weak qubit interaction to cause their substantial evolution in time—see section 6.7. If the qubit energies are different (figure 8.6c), the interaction may still be reduced, in the rotating-wave approximation, to Eq. (8.156), by compensating the energy difference  $(\Delta_1 - \Delta_2)$  with an external ac signal of frequency  $\omega = (\Delta_1 - \Delta_2)/\hbar$ —see section 6.5.

using the following product of two independent operators, plus (just for the result clarity) a common, and hence inconsequential, phase shift  $\theta' = -\pi/4$ .<sup>63</sup>

$$\hat{U}_{\text{com}} = \exp\{i\theta' (\hat{\sigma}_z^{(1)} + \hat{\sigma}_z^{(2)}) + i\theta''\} \equiv \exp\left\{i\frac{\pi}{4}\hat{\sigma}_z^{(1)}\right\} \exp\left\{i\frac{\pi}{4}\hat{\sigma}_z^{(2)}\right\} e^{-i\pi/4}. \quad (8.160)$$

Since this operator is also diagonal in the  $|j_1 j_2\rangle$  basis, it is easy to calculate the change of the basis states by the total unitary operator  $\hat{U}_{\text{tot}} \equiv \hat{U}_{\text{com}} \hat{U}_{\text{int}}$ :

$$\begin{aligned} \hat{U}_{\text{tot}}|00\rangle &= |00\rangle, & \hat{U}_{\text{tot}}|01\rangle &= |01\rangle, \\ \hat{U}_{\text{tot}}|10\rangle &= |10\rangle, & \hat{U}_{\text{tot}}|11\rangle &= -|11\rangle. \end{aligned} \quad (8.161)$$

This result already shows the main ‘miracle action’ of two-qubit gates, such as the one shown in figure 8.4b: the source qubit is left intact (only if it is in a basis state!), while the state of the target qubit is altered. True, this change (of the sign) is still different from the CNOT operator’s action (8.145), but may be readily used for its implementation by sandwiching of the transform  $U_{\text{tot}}$  between two Hadamard transforms of the target qubit alone:

$$\hat{C} = \frac{1}{2} \hat{\mathcal{H}}^{(2)} \hat{U}_{\text{tot}} \hat{\mathcal{H}}^{(2)}. \quad (8.162)$$

So, we have spent quite a bit of time on the discussion of the CNOT gate<sup>64</sup>, and now I can reward the reader for his/her effort with a bit of good news: it has been proved that an *arbitrary* unitary transform that satisfies Eq. (8.140), i.e. may be used within the general scheme outlined in figure 8.3, may be decomposed into a set of CNOT gates, possibly augmented with simpler single-qubit gates—for example, the Hadamard gate plus the  $\pi/2$  rotation discussed above<sup>65</sup>. Unfortunately, I have no time for a detailed discussion of more complex circuits<sup>66</sup>. The most famous of them is the scheme for integer number factoring, suggested in 1994 by P Shor<sup>67</sup>. Due to its potential practical importance for breaking broadly used communication encryption

<sup>63</sup> It Eq. (4.175) shows, each of component unitary transforms  $\exp\{i\theta'\hat{\sigma}_z\}$  may be created by applying to each qubit, for a time period  $\mathcal{T} = \hbar\theta'/\kappa'$ , a constant external field described by Hamiltonian  $\hat{H} = -\kappa'\hat{\sigma}_z$ . We already know that for a charged, spin- $1/2$  particle, this Hamiltonian may be created by applying  $z$ -oriented external constant magnetic field—see Eq. (4.163). For most other physical implementations of qubits, the organization of such Hamiltonian is also straightforward—see, e.g. figure 7.4 and its discussion.

<sup>64</sup> As was discussed above, this gate is identical to the two-qubit gate shown in figure 8.5a for  $f=f_3$ , i.e.  $f(j)=j$ . The implementation of the gate of  $f$  for 3 other possible functions  $f$  requires straightforward modifications, whose analysis is left for reader’s exercise.

<sup>65</sup> This fundamental importance of the CNOT gate was perhaps a major reason why D Wineland, the leader of the NIST group that had demonstrated its first experimental implementation in 1995 (following the theoretical suggestion by J Cirac and P Zoller), was awarded the 2012 Nobel Prize in Physics—shared with S Haroche, the leader of another group working towards quantum computation.

<sup>66</sup> For that, the reader may be referred to either the monographs by Nielsen–Chuang and Reiffel–Polak, cited above, or to a shorter (but much more formal) textbook [10].

<sup>67</sup> A clear description of this algorithm may be found in several accessible sources, including *Wikipedia*—see the article *Shor’s Algorithm*.

schemes such as the RSA code<sup>68</sup>, this opportunity has incited a huge wave of enthusiasm, and triggered experimental efforts to implement quantum gates and circuits using a broad variety of two-level quantum systems. By now, the following experimental options have given most significant results<sup>69</sup>:

(i) *Trapped ions*. The first experimental demonstrations of quantum state manipulation (including the already mentioned first CNOT gate) have been carried out using deeply cooled atoms in optical traps, similar to those used in frequency and time standards. Their total spins are natural qubits, whose states may be manipulated using the Rabi transfers excited by suitably tuned lasers. The spin interactions with the environment may be very weak, resulting in large dephasing times  $T_2$ —up to a few seconds. Since the distances between ions in the traps are relatively large (of the order of a micron), their direct spin–spin interaction is even weaker, but the ions may be made effectively interacting either via their mechanical oscillations about the potential minima of the trapping field, or via photons in external electromagnetic resonators (‘cavities’)<sup>70</sup>. Perhaps the main challenge of using this approach for quantum computation is a poor ‘scalability’, i.e. the enormous experimental difficulty of creating large, ordered systems of individually addressable qubits. So far, only a-few-qubit systems have been demonstrated<sup>71</sup>.

(ii) *Nuclear spins* are also typically very weakly connected to environment, with dephasing times  $T_2$  exceeding 10 s in some cases. Their eigenenergies  $E_0$  and  $E_1$  may be split by external dc magnetic fields (typically, of the order of 10 T), while the interstate Rabi transfers may be readily achieved by using the nuclear magnetic resonance, i.e. the application of external ac fields with frequencies  $\omega = (E_1 - E_0)/\hbar$ —typically, of a few hundred MHz. The challenges of this option include the weakness of spin–spin interactions (typically mediated through molecular electrons), resulting in a very slow spin evolution, whose time scale  $\hbar/\kappa$  may become comparable with  $T_2$ , and also very small level separations  $E_1 - E_0$ , corresponding to a few K, i.e. much smaller than the room temperature, creating a challenge of qubit state preparation<sup>72</sup>. Despite these challenges, the nuclear spin option was used for the first implementation of the Shor algorithm for factoring of a small number ( $15 = 5 \times 3$ ) as early as in 2001<sup>73</sup>. However, the extension of this success to larger systems, beyond the set of spins inside one molecule, is extremely challenging.

<sup>68</sup> Named after R Rivest, A Shamir, and L Adleman, the authors of the first open publication of the code in 1977, but actually invented earlier (in 1973) by C Cocks.

<sup>69</sup> For a discussion of other possible implementations (such as quantum dots and dopants in crystals) see, e.g. [11], and references therein.

<sup>70</sup> A brief discussion of such interactions (so-called Cavity QED) will be given in section 9.4 below.

<sup>71</sup> See, e.g. [12]. Note also the related work on arrays of trapped, optically-coupled neutral atoms—see, e.g. [13] and references therein.

<sup>72</sup> This challenge may be partly mitigated using ingenious spin manipulation techniques such as *refocusing*—see, e.g. either section 7.7 in Nielsen and Chuang, or the J Keeler’s monograph cited in the end of section 6.5.

<sup>73</sup> [14].

(iii) *Josephson-junction devices*. Much better scalability may be achieved with solid state devices, especially using superconductor integrated circuits including weak contacts—Josephson junctions (see their brief discussion in section 1.6). The qubits of this type all based on the fact that the energy  $U$  of such a junction is a highly nonlinear function of the Josephson phase difference  $\varphi$ —see section 1.6. Indeed, combining Eqs. (1.73) and (1.74), we can readily calculate  $U(\varphi)$  as the work  $\mathcal{W}$  of an external circuit increasing the phase from, say, zero to some value  $\varphi$ :

$$\begin{aligned} U(\varphi) - U(0) &= \int_{\varphi'=0}^{\varphi'=\varphi} d\mathcal{W} = \int_{\varphi'=0}^{\varphi'=\varphi} IV dt = \frac{2eI_c}{\hbar} \int_{\varphi'=0}^{\varphi'=\varphi} \sin \varphi' \frac{d\varphi'}{dt} dt \\ &= \frac{2eI_c}{\hbar} (1 - \cos \varphi). \end{aligned} \quad (8.163)$$

There are several options of using this nonlinearity for creating qubits<sup>74</sup>; currently the leading option, called the *phase qubit*, is using two lowest eigenstates localized in one of the potential wells of the periodic potential (8.163). A major problem of such qubits is that at the very bottom of this well the potential  $U(\varphi)$  is almost quadratic, so that the energy levels are nearly equidistant—cf. Eqs. (2.262), (6.16), and (6.23). This is even more true for the so-called ‘transmons’ (and ‘Xmons’, and ‘Gatemons’, and several other similar devices<sup>75</sup>)—the currently used phase qubits versions, where a Josephson junction is made a part of an external electromagnetic oscillator, making its relative net nonlinearity (anharmonism) even smaller. As a result, the external rf drive of frequency  $\omega = (E_1 - E_0)/\hbar$ , used to arrange the state transforms described by Eq. (8.155), may induce simultaneous undesirable transitions to (and between) higher energy levels. This effect may be mitigated by a reduction of the ac drive amplitude, but at a price of the proportional increase of the operation time. (I am leaving a quantitative estimate of this increase for the reader’s exercise.)

Since the coupling of Josephson-junction qubits may be most readily controlled (and, very importantly, kept stable if so desired), they have been used to demonstrate the largest prototype quantum computing systems to date, despite quite modest dephasing times  $T_2$ —for purely integrated circuits, in the tens of microseconds at best, even at the operation temperatures in tens of mK. By the time of this writing (mid-2018), several groups have announced chips with more than 10

<sup>74</sup> The ‘most quantum’ option in this technology is to use Josephson junctions very weakly coupled to their dissipative environment (so that the effective resistance shunting the junction is much higher than the quantum resistance unit  $R_Q \equiv (\pi/2) \hbar/e^2 \sim 10^4 \Omega$ ). In this case, the Josephson phase variable  $\varphi$  behaves as a coordinate of a 1D quantum particle, moving in the  $2\pi$ -periodic potential (8.163), forming the energy band structure  $E(q)$  similar to those discussed in section 2.7. Both theory and experiment show that in this case, the quantum states in adjacent Brillouin zones differ by the charge of one Cooper pair  $2e$ . (This is exactly the effect responsible for the Bloch oscillations of frequency (2.252).) These two states may be used as the basis states of a *charge qubit*. Unfortunately, such a qubit is rather sensitive to random charged impurities in the junction’s vicinity, causing uncontrollable changes of its parameters, so that currently, to the best of my knowledge, this option is not actively pursued.

<sup>75</sup> For a recent review of these devices see, e.g. [15], and references therein.

qubits, but to the best of my knowledge, only their smaller subsets could be used for high-fidelity quantum operations<sup>76</sup>.

(iv) *Optical systems*, attractive because of their inherently enormous bandwidth, pose a special challenge for quantum computation: due to the virtual linearity of most electromagnetic media at reasonable light power, the implementation of qubits (i.e. two-level systems), and interaction Hamiltonians such as the one given by Eq. (8.156), is problematic. In 2001, a very smart way around this hurdle was invented<sup>77</sup>. In this *KLM scheme* (also called the ‘linear optical quantum computing’), nonlinear elements are not needed at all, and quantum gates may be composed just of linear devices (such as optical waveguides, mirrors and beam splitters), plus single-photon sources and detectors. However, estimates show that this approach requires a much larger number of physical components than those using nonlinear quantum systems such as usual qubits<sup>78</sup>, so that right now it is not very popular.

So, despite more than two decades of large-scale efforts, the progress of the quantum computing development has been rather modest. The main culprit here is the unintentional coupling of qubits to environment, leading most importantly to their state dephasing, and eventually to errors. Let me discuss this major issue in detail.

Of course, some error probability exists in classical digital logic gates and memory cells as well<sup>79</sup>. However, in this case, there is no conceptual problem with the device state measurement, so that the error may be detected and corrected in many ways; perhaps the simplest one is the so-called *majority voting*. For that, the input bit set is reproduced in several (say, three) copies and sent to three similar devices whose outputs are measured and compared. If the outputs differ, at least one of the devices has made an error. This error may be not only *detected*, but also *corrected* by taking the two coinciding outputs for the correct one. If the probability of a single device error is  $W \ll 1$ , the probability of error of one device pair is close to  $W^2$ , and that of two pairs (and hence of the whole majority voting scheme) is close to  $W^3$ . Since for the currently dominating CMOS integrated circuits,  $W$  is extremely small ( $<10^{-5}$  even for relatively complex logic blocks), even such a simple error correction circuit creates a dramatic fidelity improvement—at the cost of higher circuit complexity and consumed power.

For quantum computation, the general idea of using several devices (say, qubits) for coding the same information remains valid; however, there are two major complications, both due to the analog nature of qubit states. First, as we know from chapter 7, the dephasing effect of environment may be described as a slow random drift of the probability amplitudes  $a_j$ , leading to the deviation of the output state  $\alpha_{\text{fin}}$  from the required form (8.140), and hence to a nonvanishing probability of wrong qubit state readout—see figure 8.3. Hence the quantum error correction has to

---

<sup>76</sup> See, e.g. [16] and references therein.

<sup>77</sup> [17].

<sup>78</sup> See, e.g. [18].

<sup>79</sup> In modern integrated circuits, such ‘soft’ (runtime) errors are created mostly by the high-energy neutron component of cosmic rays, and also by the  $\alpha$ -particles emitted by radioactive impurities in silicon chips and their packaging.



protect the result not against possible random state flips  $0 \leftrightarrow 1$ , as in the classical digital computer, but against these ‘creeping’ analog errors.

Second, the qubit state is impossible to copy exactly (*clone*) without disturbing it, as follows from the following simple calculation<sup>80</sup>. Cloning some state  $\alpha$  of one qubit to another qubit that is initially in an independent state (say, the basis state  $0$ ), without any change of  $\alpha$ , means the following transformation of the two-qubit ket:  $|\alpha 0\rangle \rightarrow |\alpha\alpha\rangle$ . If we want such a transform to be performed by a real quantum system whose operation is described by a unitary operator  $\hat{u}$ , and to be correct for an arbitrary state  $\alpha$ , it has to work not only for both basis states of the qubit:

$$\hat{u}|00\rangle = |00\rangle, \quad \hat{u}|10\rangle = |11\rangle, \tag{8.164}$$

but also for their arbitrary linear combination (8.133). Since the operator  $\hat{u}$  has to be linear, we may use that relation, and then Eq. (8.164) to write

$$\begin{aligned} \hat{u}|\alpha 0\rangle &\equiv \hat{u}(a_0|0\rangle + a_1|1\rangle)|0\rangle \equiv a_0\hat{u}|00\rangle + a_1\hat{u}|10\rangle \\ &= a_0|00\rangle + a_1|11\rangle. \end{aligned} \tag{8.165}$$

On the other hand, the desired result of the state cloning is

$$\begin{aligned} |\alpha\alpha\rangle &= (a_0|0\rangle + a_1|1\rangle)(a_0|0\rangle + a_1|1\rangle) \\ &\equiv a_0^2|00\rangle + a_0a_1(|10\rangle + |01\rangle) + a_1^2|11\rangle, \end{aligned} \tag{8.166}$$

i.e. is evidently different, so that, for an arbitrary state  $\alpha$ , and an arbitrary unitary operator  $\hat{u}$ ,

$$\hat{u}|\alpha 0\rangle \neq |\alpha\alpha\rangle, \tag{8.167}$$

meaning that the qubit state cloning is indeed impossible<sup>81</sup>.

This problem may be partly circumvented—for example, in the way shown in figure 8.7a. Here the CNOT gate, whose action is described by Eq. (8.145), entangles an arbitrary input state (8.133) of the source qubit with a basis initial state of an

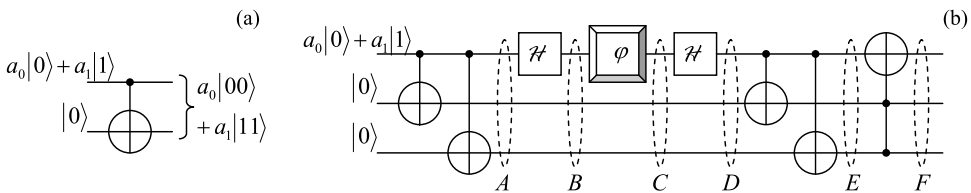


**Figure 8.7.** (a) Quasi-cloning, and (b) detection and correction of dephasing errors in a single qubit.

<sup>80</sup> Amazingly, this simple *no-cloning theorem* was discovered as late as in 1982 (to the best of my knowledge, independently by W Woiters and W Zurek, and by D Dieks), in the context of work toward quantum cryptography—see below.

<sup>81</sup> Note that this does not mean that the two (or several) qubits cannot be put into the same, arbitrary quantum state—theoretically, with arbitrary precision. Indeed, they may be first set into their lowest-energy stationary states, and then driven into the same arbitrary state (8.133) by exerting on them similar classical external fields. So, the no-cloning theorem pertains only to qubits in *unknown* states  $\alpha$ —but this is exactly what we need for error correction—see below.

ancillary target qubit—frequently called the *ancilla*. Using Eq. (8.145), we may readily calculate the output two-qubit state's vector:

$$\begin{aligned} |\alpha\rangle_{N=2} &= \hat{C}(a_0|0\rangle + a_1|1\rangle)|0\rangle \equiv a_0\hat{C}|00\rangle + a_1\hat{C}|10\rangle \\ &= a_0|00\rangle + a_1|11\rangle. \end{aligned} \quad (8.168)$$

We see that this circuit does perform the operation (8.165), i.e. gives the initial source qubit's probability amplitudes  $a_0$  and  $a_1$  equally to two qubits, i.e. duplicates the input information. However, in contrast with the 'genuine' cloning, it changes the state of the source qubit as well, making it entangled with the target (ancilla) qubit. Such 'quasi-cloning' is the key element of most suggested quantum error correction techniques.

Consider, for example, the three-qubit 'circuit' shown in figure 8.7b, which uses two ancilla qubits (see two lower lines). At its first two stages, the double application of the quasi-cloning produces an intermediate state  $A$  with the following ket-vector:

$$|A\rangle = a_0|000\rangle + a_1|111\rangle, \quad (8.169)$$

which is an evident generalization of Eq. (8.168).<sup>82</sup> Next, subjecting the source qubit to the Hadamard transform (8.146), we get the three-qubit state  $B$  represented by the vector

$$|B\rangle = a_0\frac{1}{\sqrt{2}}(|0\rangle + |1\rangle)|00\rangle + a_1\frac{1}{\sqrt{2}}(|0\rangle - |1\rangle)|11\rangle. \quad (8.170)$$

Now let us assume that at this stage, the source qubit comes into a contact with a dephasing environment (in figure 8.7b, symbolized by the single-qubit 'gate'  $\varphi$ ). As we know from section 7.3, its effect (besides some inconsequential shift of the *common* phase) may be described by a random *mutual* phase shift of the basis states<sup>83</sup>:

$$|0\rangle \rightarrow e^{i\varphi}|0\rangle, \quad |1\rangle \rightarrow e^{-i\varphi}|1\rangle. \quad (8.171)$$

As a result, for the intermediate state  $C$  (see figure 8.7b) we may write

$$\begin{aligned} |C\rangle &= a_0\frac{1}{\sqrt{2}}(e^{i\varphi}|0\rangle + e^{-i\varphi}|1\rangle)|00\rangle \\ &\quad + a_1\frac{1}{\sqrt{2}}(e^{i\varphi}|0\rangle - e^{-i\varphi}|1\rangle)|11\rangle. \end{aligned} \quad (8.172)$$

At this stage, in this simple theoretical model, the coupling with environment is completely stopped (ahhh, if this could be possible! we might have quantum

<sup>82</sup> Such a state is also the 3 qubit example of the so-called *Greenberger–Horne–Zeilinger* (GHZ) states, which are frequently called the 'most entangled' states of a system of  $N > 2$  qubits.

<sup>83</sup> For example, in the Hilbert space of this qubit, the model Hamiltonian (7.70), which was explored in section 7.3, is diagonal in the  $z$ -basis of states 0 and 1, so that the unitary transform it provides is also diagonal, giving phase shifts described by Eq. (8.171). Let me emphasize again that Eq. (8.171) is strictly valid only if the interaction with environment is a pure dephasing, i.e. does not include the energy relaxation of the qubit or its thermal activation to the higher eigenstate; however, it is a reasonable description of errors at  $T_2 \ll T_1$ .

computers by now :-), and the source qubit is fed into one more Hadamard gate. Using Eqs. (8.146) again, for the state  $D$  after this gate we get

$$|D\rangle = a_0(\cos\varphi|0\rangle + i\sin\varphi|1\rangle)|00\rangle + a_1(i\sin\varphi|0\rangle + \cos\varphi|1\rangle)|11\rangle. \quad (8.173)$$

Now the qubits are passed through the second, similar pair of CNOT gates—see figure 8.7b. Using Eq. (8.145), for the resulting state  $E$  we readily get the following expression:

$$|E\rangle = a_0\cos\varphi|000\rangle + a_0i\sin\varphi|111\rangle + a_1i\sin\varphi|011\rangle + a_1\cos\varphi|100\rangle, \quad (8.174a)$$

whose right-hand side may be evidently grouped as

$$|E\rangle = (a_0|0\rangle + a_1|1\rangle)\cos\varphi|00\rangle + (a_1|0\rangle + a_0|1\rangle)i\sin\varphi|11\rangle. \quad (8.174b)$$

This is already a rather remarkable result. It shows that if we measured the ancilla qubits at the stage  $E$ , and both results corresponded to states 0, we might be 100% sure that the source qubit (which is not affected by these measurements!) is in its initial state even after the interaction with environment. The only result of an increase of this unintentional interaction (as quantified by the magnitude of the random phase shift  $\varphi$ ) is the growth of the probability,

$$W = \sin^2\varphi, \quad (8.175)$$

of getting the opposite result, which signals a dephasing-induced error in the source qubit. Such implicit measurement, without disturbing the source qubit, is called the *quantum error detection*. An even more impressive result may be achieved by the last component of the circuit, the so-called *Toffoli* (or ‘CCNOT’) *gate*, denoted by the rightmost symbol in figure 8.7b. This 3 qubit gate is conceptually similar to the CNOT gate discussed above, besides that it flips the basis state of its target qubit only if *both* its source qubits are in the state 1. (In the circuit shown in figure 8.7b, the former role is played by our source qubit, while the latter role, by the two ancilla qubits.) According to its definition, the Toffoli gate has no effect on the first parentheses in Eq. (8.174b), but flips the source qubit’s states in the second parentheses, so that for the output 3 qubit state  $F$  we get

$$|F\rangle = (a_0|0\rangle + a_1|1\rangle)\cos\varphi|00\rangle + (a_0|0\rangle + a_1|1\rangle)i\sin\varphi|11\rangle. \quad (8.176a)$$

Obviously, this result may be factored as

$$|F\rangle = (a_0|0\rangle + a_1|1\rangle)(\cos\varphi|00\rangle + i\sin\varphi|11\rangle), \quad (8.176b)$$

showing that now the source qubit is again fully unentangled from the ancilla qubits. Moreover, calculating the norm squared of the second operand, we get

$$(\cos\varphi\langle 00| - i\sin\varphi\langle 11|)(\cos\varphi|00\rangle + i\sin\varphi|11\rangle) = \cos^2\varphi + \sin^2\varphi = 1, \quad (8.177)$$

so that the final state of the source qubit *always, exactly* coincides with its initial state. This is the famous miracle of *quantum state correction*, taking place ‘automatically’—without any qubit measurements, and for any random phase shift  $\varphi$ .

The circuit shown in figure 8.7b may be further improved by adding Hadamard gate pairs, similar to that used for the source qubit, to the ancilla qubits as well. It is straightforward to show that if the dephasing is small in the sense that the  $W$  given by Eq. (8.175) is much less than 1, this modified circuit may provide a substantial error probability reduction (to  $\sim W^2$ ) even if the ancilla qubits are also subjected to a similar dephasing and the source qubits, at the same stage—i.e. between two Hadamard gates. Such perfect automatic correction of *any* error (not only an inner dephasing of a qubit and its relaxation/excitation, but also the mutual dephasing between qubits) of *any* used qubit needs even more parallelism. The first circuit of that kind, based on 9 parallel qubits, which is a natural generalization of the circuit discussed above, had been invented in 1995 by the same P Shor. Later, 5qubit circuits enabling similar error correction were suggested. (The further parallelism reduction has been proved impossible.)

However, all these results assume that the error correction circuits as such are perfect, i.e. completely isolated from the environment. In the real world this cannot be done. Now the key question is what maximum level  $W_{\max}$  of the error probability in each gate (including those in the used error correction scheme) can be automatically corrected, and how many qubits with  $W < W_{\max}$  would be required to implement quantum computers producing important results—first of all, factoring of large numbers<sup>84</sup>. To the best of my knowledge, estimates of these two related numbers have been made only for some very specific approaches, and they are rather pessimistic. For example, using the so-called *surface codes*, which employ many physical qubits for coding an informational one, and hence increase its fidelity,  $W_{\min}$  may be increased to a few times  $10^{-3}$ , but then we would need  $\sim 10^8$  physical qubits for the Shor’s algorithm implementation<sup>85</sup>. This is very far from what currently looks doable.

Because of this hard situation, the current development of quantum computing is focused on finding at least *some* problems that could be within the reach of either the existing systems, or their immediate extensions, and simultaneously would present some practical interest—a typical example of a technology in search for applications. Currently, to my knowledge, all suggested problems of this kind address properties of some simple quantum systems—such as the molecular hydrogen<sup>86</sup> or the deuteron (the deuterium’s nucleus, i.e. the proton–neutron system)<sup>87</sup>. In the simplest option of this approach, the interaction between the qubits of a system is

---

<sup>84</sup> In order to compete with the existing classical factoring algorithms, such numbers should have at least  $10^3$  bits.

<sup>85</sup> [19].

<sup>86</sup> [20].

<sup>87</sup> [21].

organized so that the system's Hamiltonian is similar to that of the quantum system of interest<sup>88</sup>.

A similar work direction (for which 'quantum system modeling' would be a more appropriate name than 'quantum computation') is pursued by the teams using schemes different from that shown in figure 8.3. Of those, the most developed is the so-called *adiabatic quantum computation*<sup>89</sup>, which drops the hardest requirement of negligible interaction with the environment. In this approach, the qubit system is first prepared in a certain initial state, and then is allowed to evolve on its own, with no effort to couple-uncouple qubits by external control signals during the evolution<sup>90</sup>. Due to the interaction with the environment, in particular the dephasing and the energy dissipation it imposes, the system eventually relaxes to a final incoherent state, which is then measured. (This recalls the scheme shown in figure 8.3, with the important difference that the transform  $U$  should not necessarily be unitary.) From numerous runs of such an experiment, the outcome statistics may be revealed. Thus, at this approach the interaction with the environment is allowed to play a certain role in the system evolution, though every effort is made to reduce it, thus slowing down the relaxation process—hence the word 'adiabatic' in the name of this approach. This slowness allows the system to exhibit some quantum properties, in particular quantum tunneling<sup>91</sup> through the energy barriers separating close energy minima in the multi-dimensional space of states. This tunneling may create a substantial difference of the finite state statistics from that in purely classical systems, where such barriers may be overcome only by thermally-activated jumps over them<sup>92</sup>.

Due to technical difficulties of the organization and precise control of long-range interaction in multi-qubit systems, the adiabatic quantum computing demonstrations so far have been limited to a few simple arrays described by the so-called *extended quantum Ising* ('spin-glass') *model*

$$\hat{H} = -J \sum_{\{j,j'\}} \hat{\sigma}_z^{(j)} \hat{\sigma}_z^{(j')} - \sum_j h_j \hat{\sigma}_z^{(j)}, \quad (8.178)$$

where the curly brackets denote the summation over pairs of close (though not necessarily closest) neighbors. Though the Hamiltonian (8.178) is the traditional playground of phase transitions theory (see, e.g. *Part SM* chapter 4), to the best of my knowledge there are not many practically important tasks that could be achieved by studying the statistics of its solutions. Moreover, even for this limited task, the

<sup>88</sup> By the moment of this writing (mid-2018), even for such specially-tailored problems, the performance of existing quantum computing systems has been still below that of classical computers—see, e.g. [22].

<sup>89</sup> Note that the qualifier 'quantum' is important in this term, to distinguish this research direction from the *classical* adiabatic (or 'reversible') computation—see, e.g. *Part SM* section 2.3 and references therein.

<sup>90</sup> Recently, some hybrids of this approach with the 'usual' scheme of quantum computation have been demonstrated, in particular, using some control of inter-bit coupling during the relaxation process—see, e.g. [23].

<sup>91</sup> As a reminder, this process was repeatedly discussed in this course, starting from section 2.3.

<sup>92</sup> A quantitative discussion of such jumps may be found in *Part SM* section 5.6.

speed of the largest experimental adiabatic quantum ‘computers’, with several hundreds of Josephson-junction qubits<sup>93</sup> is still comparable with that of classical, off-the-shelf semiconductor processors (with the dollar cost lower by many orders of magnitude), and no dramatic change of this comparison is predicted for realistic larger systems.

To summarize the current situation with the quantum computation development, it faces a very hard challenge of mitigating the effects of unintentional coupling with the environment. This problem is exacerbated by the lack of algorithms, beyond the Shor’s number factoring, that would give quantum computation a substantial advantage over the classical competition in solving real-world problems, and hence a potential customer base much broader than the communication encryption community, that would provide the field with the necessary long-term motivation and resources. So far, the leading experts in this field abstain from predictions on when the quantum computation may become a self-supporting commercial technology<sup>94</sup>.

There seem to be better prospects for another application of entangled qubit systems, namely to telecommunication cryptography<sup>95</sup>. The goal here is to replace the currently dominating classical encryption, based on the public-key RSA code mentioned above, that may be broken by factoring very large numbers, with a quantum encryption system that would be fundamentally unbreakable. The basis of this opportunity are the measurement postulate and the no-cloning theorem: if a message is carried over by a qubit, it is impossible for an eavesdropper (in cryptography, traditionally called *Eve*) to either measure or copy it faithfully, without also disturbing its state. However, as we have seen from the discussion of figure 8.7a, state *quasi*-cloning using entangled qubits is possible, so that the issue is far from being simple, especially if we want to use a publicly distributed quantum key, in some sense similar to the classical public key used at the RSA encryption.

Unfortunately, I would not have time/space to discuss various options for quantum encryption, but cannot help demonstrating how counter-intuitive they may be, on the famous example of the so-called *quantum teleportation* (figure 8.8).<sup>96</sup> Suppose that some party A (in cryptography, traditionally called *Alice*) wants to send to party B (*Bob*) the full information about the pure quantum state  $\alpha$  of a qubit, unknown to either party. Instead of sending her qubit directly to Bob, Alice asks *him*

---

<sup>93</sup> See, e.g. [24]. Similar demonstrations with trapped-ion systems so far have been on a smaller scale, with a few tens of qubits—see, e.g. [25].

<sup>94</sup> See, e.g. [26].

<sup>95</sup> This field was pioneered in the 1970s by S Wiesner. Its important theoretical aspect (which I, unfortunately, also will not be able to cover) is the distinguishability of different but close quantum states—for example, of an original qubit set, and that slightly corrupted by noise. A good introduction to this topic may be found, for example, in chapter 9 of the monograph by Nielsen and Chuang, cited above.

<sup>96</sup> This procedure had been first suggested in 1993 by the same C Bennett, and then repeatedly demonstrated experimentally—see, e.g. [27], and literature therein.

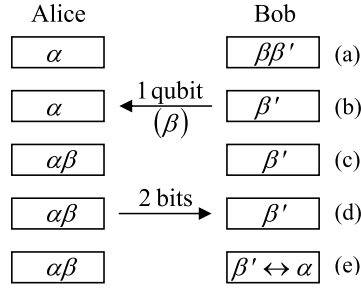


**Figure 8.8.** Sequential stages of a ‘quantum teleportation’ procedure: (a) the initial state with entangled qubits  $\beta$  and  $\beta'$ , (b) back transfer of the qubit  $\beta$ , (c) measurement of the pair  $\alpha\beta$ , (d) forward transfer of 2 classical bits with the measurement results, and (e) the final state, with the state of the qubit  $\beta'$  mirroring the initial state of the qubit  $\alpha$ .

to send *her* one qubit ( $\beta$ ) of a pair of other qubits, prepared in a certain entangled state, for example in the singlet state described by Eq. (8.11); in our current notation

$$|\beta\beta'\rangle = \frac{1}{\sqrt{2}}(|01\rangle - |10\rangle). \quad (8.179)$$

The initial state of the whole 3 qubit system may be represented in the form

$$\begin{aligned} |\alpha\beta\beta'\rangle &= (a_0|0\rangle + a_1|1\rangle)|\beta\beta'\rangle \\ &= \frac{a_0}{\sqrt{2}}|001\rangle - \frac{a_0}{\sqrt{2}}|010\rangle + \frac{a_1}{\sqrt{2}}|1010\rangle - \frac{a_1}{\sqrt{2}}|111\rangle, \end{aligned} \quad (8.180a)$$

which may be equivalently rewritten as the following linear superposition,

$$\begin{aligned} |\alpha\beta\beta'\rangle &= \frac{1}{2}|\alpha\beta\rangle_s^+ (-a_1|0\rangle + a_0|1\rangle) + \frac{1}{2}|\alpha\beta\rangle_s^- (a_1|0\rangle + a_0|1\rangle) \\ &\quad + \frac{1}{2}|\alpha\beta\rangle_e^+ (-a_0|0\rangle + a_1|1\rangle) + \frac{1}{2}|\alpha\beta\rangle_e^- (-a_0|0\rangle - a_1|1\rangle), \end{aligned} \quad (8.180b)$$

of the following four states of the qubit pair  $\alpha\beta$ :

$$|\alpha\beta\rangle_s^\pm \equiv \frac{1}{\sqrt{2}}(|00\rangle \pm |11\rangle), \quad |\alpha\beta\rangle_e^\pm \equiv \frac{1}{\sqrt{2}}(|01\rangle \pm |10\rangle). \quad (8.181)$$

After having received the qubit  $\beta$  from Bob, Alice measures which of these four states the pair  $\alpha\beta$  has. This may be achieved, for example, by measurement of one observable represented by the operator  $\hat{\sigma}_z^{(\alpha)}\hat{\sigma}_z^{(\beta)}$  and another one corresponding to  $\hat{\sigma}_x^{(\alpha)}\hat{\sigma}_x^{(\beta)}$ —cf. Eq. (8.156). (Since all four states (8.181) are eigenstates of both these operators, these two measurements do not affect each other and may be performed in any order.) The measured eigenvalue of the former operator enables distinguishing the couples of states (8.181) with different values of the lower index, while the latter measurement distinguishes the states with different upper indices.

Then Alice reports the measurement result (which may be coded with just 2 classical bits) to Bob over a classical communication channel. Since the

measurement places the pair  $\alpha\beta$  *definitely* into the corresponding state, the remaining Bob's bit  $\beta'$  is now *definitely* in the unentangled single-qubit state that is represented by the corresponding parentheses in Eq. (8.180b). Note that each of these parentheses contains both coefficients  $a_{0,1}$ , i.e. the whole information about the initial state that the qubit  $\alpha$  had initially. If Bob likes, he may now use appropriate single-qubit operations, similar to those discussed earlier in this section, to move his qubit  $\beta'$  into the state *exactly* similar to the initial state of qubit  $\alpha$ . (This fact does not violate the no-cloning theorem (8.167), because the measurement has already changed the state of  $\alpha$ .) This is of course a 'teleportation' only in a very special sense of this term, but a good example of the importance of qubit entanglement's preservation at their spatial transfer<sup>97</sup>.

Returning for just a minute to quantum cryptography: since its most common quantum key distribution protocols<sup>98</sup> require just a few simple quantum gates, whose experimental implementation is not a large technological challenge, the main focus of the current effort is on decreasing the single-photon dephasing in long electromagnetic-wave transmission channels<sup>99</sup>, with sufficiently high qubit transfer fidelity. The recent progress was rather impressive, with demonstrated transfer of entangled qubits over landlines longer than 100 km,<sup>100</sup> and over at least one satellite-based line longer than 1000 km,<sup>101</sup> and also the whole quantum key distribution over a comparable distance, though as yet at a very low rate<sup>102</sup>. Let me hope that if not the author of these notes, then their readers will see this technology used in practical secure telecommunication systems.

## 8.6 Problems

*Problem 8.1.* Prove that Eq. (8.30) indeed yields  $E_g^{(1)} = (5/4)E_H$ .

*Problem 8.2.* For a diluted gas of helium atoms in their ground state, with  $n$  atoms per unit volume, calculate its:

- (i) electric susceptibility  $\chi_e$ , and
- (ii) magnetic susceptibility  $\chi_m$ ,

and compare the results.

*Hint:* You may use the model solution of problems 6.8 and 6.14, and the results of the variational description of the helium atom's ground state in section 8.2.

<sup>97</sup> For this course, this is also a good primer for the forthcoming discussion of the *EPR paradox* and the *Bell's inequalities* in chapter 10.

<sup>98</sup> Two of them are the BB84 suggested in 1984 by C Bennett and G Brassard, and the EPRBE suggested in 1991 by A Ekert. For details, see, e.g. either section 12.6 in the repeatedly cited monograph by Nielsen and Chuang, or the review [28].

<sup>99</sup> For their quantitative discussion see, e.g. *Part EM* section 7.8.

<sup>100</sup> See, e.g. [29], and references therein.

<sup>101</sup> [30].

<sup>102</sup> [31].



*Problem 8.3.* Calculate the expectation values of the following observables:  $\mathbf{s}_1 \cdot \mathbf{s}_2$ ,  $S^2 \equiv (\mathbf{s}_1 + \mathbf{s}_2)^2$  and  $S_z \equiv s_{1z} + s_{2z}$ , for the singlet and triplet states of the system of two spins- $1/2$ , defined by Eqs. (8.18) and (8.21), directly, without using the general rule (8.48) of spin addition. Compare the results with those for the system of two classical vectors of magnitude  $\hbar/2$  each.

*Problem 8.4.* Discuss the factors  $\pm 1/\sqrt{2}$  that participate in Eqs. (8.18) and (8.20) for the entangled states of the system of two spins- $1/2$ , in terms of Clebsch–Gordan coefficients similar to those discussed in section 5.7.

*Problem 8.5.\** Use the perturbation theory to calculate the contribution into the so-called *hyperfine splitting* of the ground energy of the hydrogen atom<sup>103</sup>, due to the interaction between spins of the nucleus (proton) and the electron.

*Hint:* The proton’s magnetic moment operator is described by the same Eq. (4.115) as the electron, but with a positive gyromagnetic factor  $\gamma_p = g_p e / 2m_p \approx 2.675 \times 10^8 \text{ s}^{-1} \text{ T}^{-1}$ , whose magnitude is much smaller than that of the electron ( $|\gamma_e| \approx 1.761 \times 10^{11} \text{ s}^{-1} \text{ T}^{-1}$ ), due to the much higher mass,  $m_p \approx 1.673 \times 10^{-27} \text{ kg} \approx 1,835 m_e$ . (The  $g$ -factor of the proton is also different,  $g_p \approx 5.586$ .<sup>104</sup>)

*Problem 8.6.* In the simple case of just two similar spin-interacting particles, distinguishable by their spatial location, the famous *Heisenberg model* of ferromagnetism<sup>105</sup> is reduced to the following Hamiltonian:

$$\hat{H} = -J \hat{\mathbf{s}}_1 \cdot \hat{\mathbf{s}}_2 - \gamma \mathcal{B} \cdot (\hat{\mathbf{s}}_1 + \hat{\mathbf{s}}_2),$$

where  $J$  is the spin interaction constant,  $\gamma$  is the gyromagnetic ratio of each particle, and  $\mathcal{B}$  is the external magnetic field. Find the stationary states and eigenenergies of this system for spin- $1/2$  particles.

*Problem 8.7.* Two particles, both with spin- $1/2$ , but different gyromagnetic ratios  $\gamma_1$  and  $\gamma_2$ , are placed into external magnetic field  $\mathcal{B}$ . In addition, their spins interact as in the Heisenberg model:

$$\hat{H}_{\text{int}} = -J \hat{\mathbf{s}}_1 \cdot \hat{\mathbf{s}}_2.$$

Find the eigenstates and eigenenergies of the system<sup>106</sup>.

<sup>103</sup> This effect was discovered experimentally by A Michelson in 1881, and explained theoretically by W Pauli in 1924.

<sup>104</sup> The anomalously large value of the proton’s  $g$ -factor results from the composite quark–gluon structure of this particle. (An exact calculation of  $g_p$  remains a challenge for quantum chromodynamics.)

<sup>105</sup> It was suggested in 1926, independently by W Heisenberg and P Dirac. A discussion of temperature effects on this and other similar systems (especially the Ising model of ferromagnetism) may be found in *Part SM* chapter 4.

<sup>106</sup> For similar particles (in particular, with  $\gamma_1 = \gamma_2$ ) the problem is evidently reduced to the previous one.

*Problem 8.8.* Two similar spin- $1/2$  particles, with the gyromagnetic ratio  $\gamma$ , localized at two points separated by distance  $a$ , interact via the field of their magnetic dipole moments. Calculate the spin eigenstates and eigenvalues of the system.

*Problem 8.9.* Consider the permutation of two identical particles, each of spin  $s$ . How many different symmetric and antisymmetric spin states can the system have?

*Problem 8.10.* For a system of two identical particles with  $s = 1$ :

- (i) List all possible spin states in the uncoupled-representation basis.
- (ii) List all possible pairs  $\{S, M_S\}$  of the quantum numbers describing the states of the coupled-representation basis—see Eq. (8.48).
- (iii) Which of the  $\{S, M_S\}$  pairs describe the states symmetric, and which the states antisymmetric, with respect to the particle permutation?

*Problem 8.11.* Represent the operators of the total kinetic energy and the total orbital angular momentum of a system of two particles, with masses  $m_1$  and  $m_2$ , as combinations of terms describing the center-of-mass motion and the relative motion. Use the results to calculate the energy spectrum of the so-called *positronium*—a metastable ‘atom’<sup>107</sup> consisting of one electron and its positively charged antiparticle, the positron.

*Problem 8.12.* Two particles with similar masses  $m$  and charges  $q$  are free to move along a round, plane ring of radius  $R$ . In the limit of strong Coulomb interaction of the particles, find the lowest eigenenergies of the system, and sketch the system of its energy levels. Discuss possible effects of particle indistinguishability.

*Problem 8.13.* Low-energy spectra of many diatomic molecules may be well described modeling the molecule as a system of two particles connected with a light and elastic, but very stiff spring. Calculate the energy spectrum of a molecule in this approximation. Discuss possible effects of nuclear spins on the spectra of so-called *homonuclear* molecules, formed by two similar atoms.

*Problem 8.14.* Two indistinguishable spin- $1/2$  particles are attracting each other at contact:

$$U(x_1, x_2) = -w\delta(x_1 - x_2), \quad \text{with } w > 0,$$

but are otherwise free to move along the  $x$ -axis. Find the energy and the wavefunction of the ground state of the system.

*Problem 8.15.* Calculate the energy spectrum of the system of two identical spin- $1/2$  particles, moving along the  $x$ -axis, which is described by the following Hamiltonian:

---

<sup>107</sup> Its lifetime (either 0.124 ns or 138 ns, depending on the parallel or antiparallel configuration of the components spins), is limited by the weak interaction of its components, which causes their annihilation with the emission of several gamma-ray photons.

$$\hat{H} = \frac{\hat{p}_1^2}{2m_0} + \frac{\hat{p}_2^2}{2m_0} + \frac{m_0\omega_0^2}{2}(x_1^2 + x_2^2 + \epsilon x_1 x_2),$$

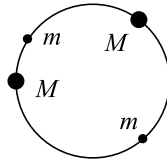
and the degeneracy of each energy level.

*Problem 8.16.\** Two indistinguishable spin- $1/2$  particles are confined to move around a circle of radius  $R$ , and interact only at a very short arc distance  $l = R\varphi \equiv R(\varphi_1 - \varphi_2)$  between them, so that the interaction potential  $U$  may be well approximated with a delta-function of  $\varphi$ . Find the ground state and its energy, for the following two cases:

- (i) the ‘orbital’ (spin-independent) repulsion:  $\hat{U} = \mathcal{W}\delta(\varphi)$ ,
- (ii) the spin–spin interaction:  $\hat{U} = -\mathcal{W}\hat{\mathbf{s}}_1 \cdot \hat{\mathbf{s}}_2 \delta(\varphi)$ ,

both with constant  $\mathcal{W} > 0$ . Analyze the trends of your results in the limits  $\mathcal{W} \rightarrow 0$  and  $\mathcal{W} \rightarrow \infty$ .

*Problem 8.17.* Two particles of mass  $M$ , separated by two much lighter particles of mass  $m \ll M$ , are placed on a ring of radius  $R$ —see figure below. The particles strongly repulse at contact, but otherwise each of them is free to move along the ring. Calculate the lower part of the energy spectrum of the system.



*Problem 8.18.*  $N$  indistinguishable spin- $1/2$  particles move in a spherically-symmetric quadratic potential  $U(\mathbf{r}) = m\omega_0^2 r^2/2$ . Neglecting the direct interaction of the particles, find the ground-state energy of the system.

*Problem 8.19.* Use the Hund rules to find the values of the quantum numbers  $L$ ,  $S$ , and  $J$  in the ground states of the atoms of carbon and nitrogen. Write down the Russell–Saunders symbols for these states.

*Problem 8.20.*  $N \gg 1$  indistinguishable, non-interacting quantum particles are placed in a hard-wall, rectangular box with sides  $a_x$ ,  $a_y$ , and  $a_z$ . Calculate the ground-state energy of the system, and the average forces it exerts on each face of the box. Can we characterize the forces by certain pressure  $\mathcal{P}$ ?

*Hint:* Consider separately the cases of bosons and fermions.

*Problem 8.21.\** Explore the *Thomas–Fermi model*<sup>108</sup> of a heavy atom, with the nuclear charge  $Q = Ze \gg e$ , in which the interaction between electrons is limited to their contribution to the common electrostatic potential  $\phi(\mathbf{r})$ . In particular, derive

<sup>108</sup> It was suggested in 1927, independently, by L Thomas and E Fermi.

the ordinary differential equation obeyed by the radial distribution of the potential, and use it to estimate the effective radius of the atom.

*Problem 8.22.\** Use the Thomas–Fermi model, explored in the previous problem, to calculate the total binding energy of a heavy atom. Compare the result with that for the simpler model, in which the Coulomb electron–electron interaction is completely ignored.

*Problem 8.23.* A system of three similar but distinguishable spin- $1/2$  particles is described by the Heisenberg Hamiltonian (cf. problems 8.6 and 8.7):

$$\hat{H} = -J (\hat{\mathbf{s}}_1 \cdot \hat{\mathbf{s}}_2 + \hat{\mathbf{s}}_2 \cdot \hat{\mathbf{s}}_3 + \hat{\mathbf{s}}_3 \cdot \hat{\mathbf{s}}_1),$$

where  $J$  is the spin interaction constant. Find the stationary states and eigenenergies of this system, and give an interpretation of your results.

*Problem 8.24.* For a system of three distinguishable spins- $1/2$ , find the common eigenstates and eigenvalues of the operators  $\hat{S}_z$  and  $\hat{S}^2$ , where

$$\hat{\mathbf{S}} \equiv \hat{\mathbf{s}}_1 + \hat{\mathbf{s}}_2 + \hat{\mathbf{s}}_3$$

is the vector operator of the total spin of the system. Do the corresponding quantum numbers  $S$  and  $M_S$  obey Eqs. (8.48)?

*Problem 8.25.* Explore basic properties of the Heisenberg model (which was the subject of problems 8.6, 8.7, and 8.23), for a 1D chain of  $N$  spins- $1/2$ :

$$\hat{H} = -J \sum_{\{j,j'\}} \hat{\mathbf{s}}_j \cdot \hat{\mathbf{s}}_{j'} - \gamma \mathcal{B} \cdot \sum_j \hat{\mathbf{s}}_j, \quad \text{with } J > 0,$$

where the summation is over all  $N$  spins, with the symbol  $\{j, j'\}$  meaning that the first sum is only over the adjacent spin pairs. In particular, find the ground state of the system and its lowest excited states in the absence of external magnetic field  $\mathcal{B}$ , and also the dependence of their energies on the field.

*Hint:* For the sake of simplicity, you may assume that the first sum includes the term  $\hat{\mathbf{s}}_N \cdot \hat{\mathbf{s}}_1$  as well. (Physically, this means that the chain is bent into a closed loop<sup>109</sup>.)

*Problem 8.26.* Compose the simplest model Hamiltonians, in terms of the second quantization formalism, for systems of indistinguishable particles moving in the following systems:

- (i) two weakly coupled potential wells, with on-site particle-pair interactions (giving additional energy  $J$  per each pair of particles in the same potential well), and

---

<sup>109</sup> Note that for dissipative spin systems, differences between low-energy excitations of open-end and closed-end 1D chains may be substantial even in the limit  $N \rightarrow \infty$ —see, e.g. *Part SM* section 4.5. However, for our Hamiltonian (and hence dissipation-free) system, the differences are relatively small.

- (ii) a periodic 1D potential, with the same particle-pair interactions, in the tight-binding limit.

*Problem 8.27.* For each of the Hamiltonians composed in the previous problem, derive the Heisenberg equations of motion for particle creation operators, for

- (i) bosons, and  
(ii) fermions.

*Problem 8.28.* Express the ket-vectors of all possible Dirac states for the system of three indistinguishable

- (i) bosons, and  
(ii) fermions,

via those of their single-particle states  $\beta$ ,  $\beta'$ , and  $\beta''$  they occupy.

*Problem 8.29.* Explain why the general perturbative result (8.126), when applied to the  $^4\text{He}$  atom, gives the correct<sup>110</sup> expression (8.29) for the ground singlet state, and correct Eqs. (8.39)–(8.42) (with the minus sign in the first of these relations) for the excited triplet states, but cannot describe these results, with the plus sign in Eq. (8.39), for the excited singlet state.

*Problem 8.30.* For a system of two distinct qubits (i.e. two-level systems), introduce a reasonable uncoupled-representation  $z$ -basis, and find in this basis the  $4 \times 4$  matrix of the operator that swaps their states.

*Problem 8.31.* Find a time-independent Hamiltonian that may cause the qubit evolution described by Eqs. (8.155). Discuss the relation between your result and the time-dependent Hamiltonian (6.86).

## References

- [1] Pendry J 1994 *Adv. Phys.* **43** 461
- [2] Szabo A and Ostlund N 1996 *Modern Quantum Chemistry* Revised edn (Dover)
- [3] Simonian N *et al* 2013 *J. Appl. Phys.* **113** 044504
- [4] Medvedev M *et al* 2017 *Science* **335** 49
- [5] Hutama A *et al* 2017 *J. Phys. Chem. C* **121** 14888
- [6] Parr R and Yang W 1994 *Density-Functional Theory of Atoms and Molecules* (Oxford University Press)
- [7] Stechel J and Sholl D 2009 *Density Functional Theory: Practical Introduction* (Wiley)
- [8] Zangwill A 2015 *Phys. Today* **68** 34
- [9] Nielsen M and Chuang I 2000 *Quantum Computation and Quantum Information* (Cambridge University Press)
- [10] Mermin N 2007 *Quantum Computer Science* (Cambridge University Press)

<sup>110</sup>Correct in the sense of the first order of the perturbation theory.

- [11] Ladd T *et al* 2010 *Nature* **464** 45
- [12] Debnath S *et al* 2016 *Nature* **536** 63
- [13] Perczel J *et al* 2017 *Phys. Rev. Lett.* **119** 023603
- [14] Lanyon B *et al* 2001 *Phys. Rev. Lett.* **99** 250505
- [15] Wendin G 2017 *Progr. Rep. Phys* **80** 106001
- [16] Song C *et al* 2017 *Phys. Rev. Lett.* **119** 180511
- [17] Knill E *et al* 2001 *Nature* **409** 46
- [18] Li Y *et al* 2015 *Phys. Rev. X* **5** 041007
- [19] Fowler A *et al* 2012 *Phys. Rev. A* **86** 032324
- [20] O'Malley P *et al* 2016 *Phys. Rev. X* **6** 031007
- [21] Dumitrescu E *et al* 2018 *Phys. Lett. Lett* **120** 210501
- [22] Chen J *et al* 2018 arXiv: 1805.01450v2
- [23] Barends R *et al* 2016 *Nature* **534** 222
- [24] Harris R *et al* 2018 *Science* **361** 162
- [25] Zhang J *et al* 2017 *Nature* **551** 601
- [26] National Academies of Sciences, Engineering, and Medicine 2019 *Quantum Computing: Progress and Prospects* (Washington, DC: The National Academies Press)
- [27] Steffen L *et al* 2013 *Nature* **500** 319
- [28] Gisin N *et al* 2002 *Rev. Mod. Phys.* **74** 145
- [29] Herbst T *et al* 2015 *Proc. Natl. Acad. Sci.* **112** 14202
- [30] Yin J *et al* 2017 *Science* **356** 1140
- [31] Yin H-L *et al* 2016 *Phys. Rev. Lett.* **117** 190501